An Unfitted Finite Element Method for the Dynamic Landau–de Gennes Model of Nematic Liquid Crystals

Jeremy T. Shahan
Department of Mathematics
Louisiana State University,
Baton Rouge, LA 70803-4918, U.S.A.
Email: jshaha2@lsu.edu

Shawn W. Walker
Department of Mathematics
Louisiana State University,
Baton Rouge, LA 70803-4918, U.S.A.
Email: walker@math.lsu.edu

Abstract

We develop an unfitted finite element method for simulating the dynamic Landau–de Gennes (LdG) Q-tensor model in moving domains. The model is partially based on the Beris–Edwards system, except the fluid velocity is prescribed. This leaves a dynamic equation for the evolution of Q that involves the corotational derivative. The motivating application is simulating the dynamics of colloidal bodies immersed in a liquid crystal.

We establish unique solvability and stability for the semi-discrete and fully discrete finite element schemes, which use Nitsche's method and stabilization for cut elements. In particular, we extend unfitted techniques to handle nonlinear parabolic equations, with tensor-valued solutions, in time-dependent domains. Moreover, we provide a convergence analysis that accounts for both geometric and PDE error contributions.

Numerical experiments are presented that demonstrate the method's accuracy and flexibility in capturing defect structures and colloid-colloid interactions under varying anchoring (i.e. boundary) conditions.

Keywords— liquid crystal, unfitted finite element method, Beris–Edwards, colloid

1 Introduction

Liquid crystals (LCs) are an anisotropic material that exhibits long-range orientational order which yields interesting optical properties and easy modulation by external fields (e.g. electric or magnetic) [16, 21, 28]. Moreover, colloidal particles immersed in an LC act as inclusions that induce local distortions and defects in the medium and present a rich landscape of physical phenomena [2, 31, 40]. These effects are not only of fundamental interest in soft matter physics but also have practical importance for the design of responsive materials, photonic devices, and self-assembled structures [13, 14, 38].

In this paper, we consider the time-dependent Landau–de Gennes (LdG) Q-tensor theory, which captures both the orientational order and the formation of topological defects [45, 49, 37]. Colloidal objects are treated as rigid bodies immersed in the LC (i.e. inclusions) with prescribed anchoring (boundary) conditions on their surfaces, which influence the surrounding director field and give rise to elastic distortions and topological defect structures [40]. Furthermore, the colloidal particles *move with a prescribed motion* as a first step toward modeling the full dynamics of self-assembling colloids [6, 42, 48].

The main contribution of this paper is the development of an unfitted finite element method (FEM) for simulating these systems. A traditional mesh-based approach would require complex or costly remeshing to conform to the moving geometry of the immersed colloids [8, 1, 3, 29]. On the other hand, our unfitted scheme allows the colloid boundaries to be embedded within a fixed background mesh using level set functions to represent the colloids [11, 10, 34]. The formulation requires penalization of boundary conditions (e.g. Nitsche's method) as well as stabilization of cut elements, but this is fairly well understood now [9, 24, 12]. The unfitted approach allows flexible handling of complex geometric motion of interfaces, while maintaining high accuracy and stability in the numerical solution.

Our variational formulation of the dynamic LdG system involves half of the so-called Beris–Edwards system [5, 51]. As a simplification, we assume the colloid motion is prescribed and that the resulting velocity field of the LC medium is also prescribed. Thus, the Navier–Stokes part of Beris–Edwards is not needed. This leaves the dynamic Q-tensor equation which involves the corotational derivative of Q that is required to maintain objectivity [23, 45]. Therefore, another contribution of this paper is to extend unfitted FEM techniques to handle non-linear, parabolic systems with complex boundary conditions. Moreover, our method provides a test-bed for investigating defect-mediated interactions, colloid alignment, and the role of confinement and boundary geometry in directing LC behavior. Hence, this work should be useful for applications.

The paper is outlined as follows. Section 2 reviews the Landau–de Gennes model of LCs, including the dynamic Beris–Edwards model when the fluid velocity field is prescribed, and the weak formulation of the model. In Section 3, we first consider a time discretization of the dynamic model but no spatial discretization and we establish unique solvability and stability of the semi-discrete method; we highlight that the stability estimate is *not* exponential in the final time T. Next, we consider the fully discrete problem in Section 4 where we use unfitted techniques to handle the spatial discretization. The details of the unfitted method are described and stability is established. Section 5 provides the error analysis of our scheme which accounts for both the geometric error and the usual "PDE error." Several numerical experiments are given in Section 6 that demonstrate the effectiveness of our scheme that show defect structures and colloid–colloid interactions with different anchoring conditions. We conclude in Section 7 with some remarks and future outlook.

2 The Landau–de Gennes Model

2.1 Order Parameter

The material representation of liquid crystals (LCs) uses a mesoscopic, tensor-valued order parameter Q [16]. It is symmetric and traceless and, in three dimensions, Q belongs to [15]

$$\mathbf{S}_0 := \{Q \in \mathbb{R}^{3\times 3} \mid Q^\dagger = Q,\ \operatorname{tr}(Q) = 0\}. \tag{1}$$

The order parameter Q is related to the covariance matrix for the probability distribution of the orientation of LC molecules. It can be shown that [49, 37], in three dimensions, the eigenvalues of Q lie in the range $[-1/3, 2/3]$.

When all eigenvalues are equal, they vanish and $Q = 0$, which represents the isotropic state (a uniformly random distribution of LC molecule orientations). If all eigenvalues are distinct, then Q is in a *biaxial* state. Most nematic LCs have a preferred state of a single largest eigenvalue with the other two eigenvalues equal; this is called a *uniaxial* state and Q has the form

$$Q = s\left(\mathbf{n}\otimes\mathbf{n} - \frac{1}{3}I\right), \tag{2}$$

where $\mathbf{n}$ satisfies $|\mathbf{n}| = 1$ and is the eigenvector for the dominant (distinct) eigenvalue. The vector is called the *director* and represents the main average direction in which the LC molecules are pointing. The scalar order parameter $s \in [-1/2, 1]$ is called the *degree-of-orientation* and is a measure of the orientational order of the LC molecules, i.e. how well aligned they are with $\mathbf{n}$.

2.2 Free Energy

We let $\Omega \subset \mathbb{R}^3$ be the domain of the LC material, and is time-dependent, where $Q : \Omega \to \mathbf{S}_0$ is a tensor-valued function that specifies the state of the LCs throughout the domain. We assume Ω has Lipschitz boundary Γ

with outward pointing unit normal vector $\boldsymbol{\nu}$. The free energy of the LdG model is defined as [36, 37, 40, 27]:

$$E[Q] := \int_\Omega f(Q, \nabla Q)\, d\mathbf{x} + \int_\Omega \psi(Q)\, d\mathbf{x} + \int_\Gamma g(Q)\, dS(\mathbf{x}) + \int_\Gamma \phi(Q)\, dS(\mathbf{x}) - \int_\Omega \chi(Q)\, d\mathbf{x}, \tag{3}$$

with the elastic energy given by

$$f(Q, \nabla Q) := \frac{1}{2}\Big(\ell_1|\nabla Q|^2 + \ell_2|\nabla\cdot Q|^2 + \ell_3(\nabla Q)^\dagger \,\vdots\, \nabla Q + 4\ell_1\tau_0 \nabla Q \,\vdots\, (\varepsilon\cdot Q)\Big), \tag{4}$$

where $\{\ell_i\}_{i=1}^3$ (units of $\mathrm{J}\cdot\mathrm{m}^{-1}$) and τ_0 (units of m^{-1}) are material dependent elastic constants, where τ_0 models cholesteric twist. More specifically,

$$\begin{aligned} |\nabla Q|^2 &:= Q_{ij,k}Q_{ij,k}, \quad |\nabla\cdot Q|^2 := Q_{ij,j}Q_{ik,k}, \\ (\nabla Q)^\dagger \,\vdots\, \nabla Q &:= Q_{ij,k}Q_{ik,j}, \quad \nabla Q \,\vdots\, (\varepsilon\cdot Q) := \varepsilon_{jkl}Q_{ik,l}Q_{ij} = -(\nabla\times Q) : Q, \end{aligned} \tag{5}$$

where we use the convention of summation over repeated indices, ε_{jkl} is the Levi-Civita tensor, and $(\nabla\times Q)_{ij} := \varepsilon_{j\ell k}Q_{ik,\ell}$ is the row-wise curl of Q. Note that taking $\ell_i = 0$, for $i = 2, 3$, and $\tau_0 = 0$ gives the often used one-constant LdG model. More complicated models can also be considered [37, 16, 45].

Next, the bulk potential ψ is a double-well type of function that is given by

$$\psi(Q) = a_0 - \frac{a_2}{2}\mathrm{tr}(Q^2) - \frac{a_3}{3}\mathrm{tr}(Q^3) + \frac{a_4}{4}\big(\mathrm{tr}(Q^2)\big)^2, \tag{6}$$

which governs the isotropic-to-nematic phase transistion. Above, a_2, a_3, a_4 are material parameters (units of $\mathrm{J}\cdot\mathrm{m}^{-3}$) such that a_2, a_3, a_4 are positive; a_0 is a convenient constant to ensure $\psi \geq 0$. Stationary points of ψ are either uniaxial or isotropic Q-tensors [45].

The surface energy, composed of the quadratic $g(Q)$ and higher-order boundary potential $\phi(Q)$, accounts for *weak anchoring* of the LC (i.e. penalization of boundary conditions). For example, a Rapini-Papoular type anchoring energy [4] can be considered:

$$g(Q) = \frac{w_0}{2}|Q - Q_\Gamma|^2 + \frac{w_1}{2}|\widetilde{Q} - \widetilde{Q}^\perp|^2, \quad \phi(Q) = \frac{w_2}{4}\left(|\widetilde{Q}|^2 - s_0^2\right)^2, \tag{7}$$

where w_0, w_1, and w_2 are positive constants (units of $\mathrm{J}\cdot\mathrm{m}^{-2}$), $Q_\Gamma(x) \in \mathbf{S}_0$ for all $\boldsymbol{x} \in \Gamma$, and s_0 is the scalar order parameter of the uniaxial Q that minimizes the double well. We set $\widetilde{Q} := Q + \frac{s_0}{3}I$, and define the standard projection onto the plane orthogonal to $\boldsymbol{\nu}$, that is, $Q^\perp := \Pi Q \Pi$ where $\Pi = I - \boldsymbol{\nu}\otimes\boldsymbol{\nu}$. We define Q_Γ to be uniaxial of the form

$$Q_\Gamma = s_0\left(\boldsymbol{\nu}\otimes\boldsymbol{\nu} - \frac{1}{3}I\right). \tag{8}$$

The w_0 term in (7) models homeotropic (normal) anchoring, while w_1 and w_2 model planar degenerate anchoring.

For the analysis, we modify the quartic term to have quadratic growth. Let $\rho : [0,\infty) \to \mathbb{R}_+$ be a smooth cut-off function, i.e.

$$\begin{cases} \rho(r) = 1 & \text{if } r < b_1, \\ \rho(r) = \text{ monotone} & \text{if } b_1 \leq r \leq b_2, \\ \rho(r) = 0 & \text{if } r > b_2, \end{cases}$$

where $1 \leq b_1 < b_2$ are fixed constants. We then modify the boundary potential

$$\tilde{\phi}(Q) = \phi(Q)\rho(|Q|^2) + w_2^2|Q|^2\left(1 - \rho(|Q|^2)\right), \tag{9}$$

which then implies the following estimates

$$|\tilde{\phi}(Q)| \leq \frac{w_2 s_0^4}{4} + c_0|Q|^2, \qquad |\tilde{\phi}'(Q)| \leq c_1|Q|, \qquad |\tilde{\phi}''(Q)| \leq c_2, \tag{10}$$

where c_0, c_1, and c_2 are positive constants. For the remainder of the paper, we omit the tilde and simply write ϕ.

The function $\chi(\cdot)$ models external forcing on the LC system which can arise due to an external electric or magnetic field. Usually, $\chi(Q)$ is taken to be linear in Q, i.e. $\chi(Q) = U_\Omega : Q$, where $U_\Omega : \Omega \to \mathbb{R}^{3\times 3}$ is a given function.

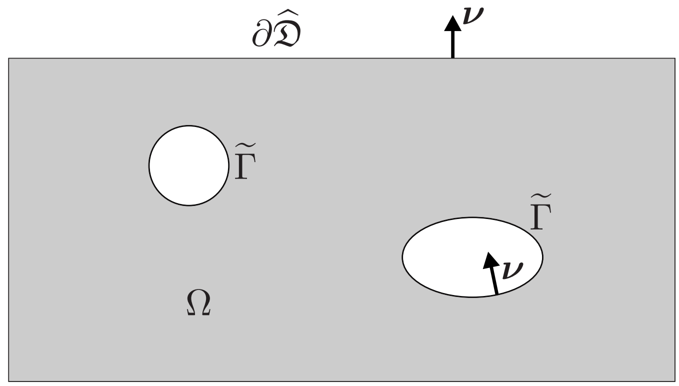

Figure 1: Diagram of the liquid crystal domain $\Omega(t)$. The boundary partitions as $\partial\Omega(t) \equiv \Gamma(t) = \partial\widehat{\mathfrak{D}} \cup \widetilde{\Gamma}(t)$, where $\widetilde{\Gamma}(t)$ indicates the actively moving parts of the boundary.

2.3 Time-dependent Flow

Since the domain $\Omega = \Omega(t)$ is time-dependent, and the LC state $Q = Q(t, \boldsymbol{x})$ changes with time, we consider an evolution equation for Q that is motivated from the Beris–Edwards system [52]. The domain evolution is assumed to be bounded $\Omega(t) \subset \widehat{\mathfrak{D}}$ for all t, and the outer boundary $\partial\Omega(t) \cap \partial\widehat{\mathfrak{D}} \equiv \partial\widehat{\mathfrak{D}}$ does not change with t (see Figure 1). Indeed, $\Gamma(t) := \partial\Omega(t) = \partial\widehat{\mathfrak{D}} \cup \widetilde{\Gamma}(t)$, where $\widetilde{\Gamma}(t) \in C^{m+1}$, for some $m \geq 1$, is the smooth inner boundary. The outer boundary, $\partial\widehat{\mathfrak{D}}$, is assumed to be piecewise C^2 and Lipschitz and is stationary.

Moreover, we assume there exists a diffeomorphism $\Psi : \widehat{\mathfrak{D}} \to \widehat{\mathfrak{D}}$ such that $\Omega(t) = \Psi(\Omega_{\text{ref}})$, where Ω_{ref} is a fixed reference domain, and $\Psi \in C^{m+1}([0,T] \times \widehat{\mathfrak{D}})$. With this, we define the material velocity $\mathbf{v}(t, \cdot)$ of $\Omega(t)$ via

$$\mathbf{v}(t, \Psi(t, \mathbf{y})) := \partial_t \Psi(t, \mathbf{y}), \quad \text{for all } t \in [0,T], \text{ and all } \mathbf{y} \in \widehat{\mathfrak{D}},$$

and we assume further that $\mathbf{v}$ is divergence free. Note that the strain and vorticity tensor, respectively, are given by

$$S = S(\nabla\mathbf{v}) := \frac{\nabla\mathbf{v} + (\nabla\mathbf{v})^\dagger}{2}, \quad W = W(\nabla\mathbf{v}) := \frac{\nabla\mathbf{v} - (\nabla\mathbf{v})^\dagger}{2}. \tag{11}$$

Next, we define the notion of non-cylindrical space-time domain for posing the PDE. To this end, let

$$\mathcal{C} = \cup_{t\in(0,T)}\{t\} \times \Omega(t), \quad \mathcal{O}(\mathcal{C}) = \cup_{t\in(0,T)}\{t\} \times \mathcal{O}(\Omega(t)), \quad \mathcal{C} \subset \mathcal{O}(\mathcal{C}) \subset \mathbb{R}^3, \tag{12}$$

where $\mathcal{O}(D)$ is an open neighborhood containing the set D; similarly, we also have $\mathcal{G} = \cup_{t\in(0,T)}\{t\} \times \partial\Omega(t)$. Then, $Q(t, \boldsymbol{x})$ satisfies the following parabolic system on $\mathcal{C}$:

$$\begin{aligned} \partial_t Q + (\mathbf{v} \cdot \nabla)Q + \frac{1}{t_0}\widehat{\frac{\delta E}{\delta Q}} &= B(\nabla\mathbf{v}, Q) + \frac{2p_0}{3}S, \\ B(\nabla\mathbf{v}, Q) &:= WQ - QW + p_0(QS + SQ) - 2p_0(S : Q)(Q + I/3), \end{aligned} \tag{13}$$

where t_0 is the relaxation time, $p_0 \in [-1,1]$ is a material parameter, $\widehat{\cdot}$ is the symmetric traceless part of a tensor, and the boundary conditions come from the weak anchoring conditions. We call $B(\nabla\mathbf{v}, Q)$ the modified Beris–Edwards term and note that $B(\nabla\mathbf{v}, Q) + \frac{2p_0}{3}S$ is symmetric and trace-free.

Next, we non-dimensionalize the PDE. In particular, we note that the dimensional $\psi'(Q)$ is replaced by $\eta^{-2}\psi'(Q)$, where $\eta > 0$ and $|\psi'(Q)| = O(1)$; similarly, the dimensional $\phi'(Q)$ is replaced by $\omega^{-1}\phi'(Q)$, where $\omega > 0$ and $|\phi'(Q)| = O(1)$. Then, taking $t_0 = 1$ for simplicity, the full strong form is given by

$$\begin{aligned} \partial_t Q + (\mathbf{v} \cdot \nabla)Q - 4\ell_1\tau_0\widehat{\nabla \times Q} - B(\nabla\mathbf{v}, Q) - \operatorname{div}\widehat{(\mathcal{A}\nabla Q)} + \frac{1}{\eta^2}\widehat{\psi'(Q)} &= \widehat{U_\Omega} + \frac{2p_0}{3}S, && \text{in } \mathcal{C}, \\ \widehat{\partial_{\boldsymbol{\nu}_\mathcal{A}} Q} + 2\ell_1\tau_0\widehat{\boldsymbol{\nu} \times Q} + w_0(Q - Q_\Gamma) + w_1(\widehat{\widetilde{Q} - \widetilde{Q}^\perp}) + \frac{1}{\omega}\widehat{\phi'(Q)} &= 0, && \text{on } \mathcal{G}, \\ Q(0, \boldsymbol{x}) &= Q_0, && \text{on } \Omega(0), \end{aligned} \tag{14}$$

where $(\boldsymbol{\nu} \times Q)_{ij} := \varepsilon_{jlk}\nu_l Q_{ik}$ (row-wise cross product) and $\mathcal{A}$ is a 6-tensor such that

$$a_{\mathrm{e}}(\Omega; Q, P) := \ell_1 (Q_{ij,k}, P_{ij,k})_\Omega + \ell_2 (Q_{ij,j}, P_{ik,k})_\Omega + \ell_3 (Q_{ij,k}, P_{ik,j})_\Omega \equiv (\mathcal{A}\nabla Q, \nabla P)_\Omega\,, \tag{15}$$

$$a_{\mathrm{t}}(\Omega; Q, P) := 2\ell_1\tau_0 \left[\varepsilon_{ikl} (Q_{jk,l}, P_{ij})_\Omega + \varepsilon_{ikl} (P_{jk,l}, Q_{ij})_\Omega\right] \equiv -2\ell_1\tau_0 \left[(\nabla \times Q, P)_\Omega + (\nabla \times P, Q)_\Omega\right], \tag{16}$$

and

$$[\mathrm{div}\,(\mathcal{A}\nabla Q)]_{ij} = \ell_1 Q_{ij,kk} + (\ell_2 + \ell_3) Q_{ik,jk}, \quad [\partial_{\boldsymbol{\nu}_\mathcal{A}} Q]_{ij} = \ell_1 \nu_k Q_{ij,k} + \ell_2 \nu_j Q_{ik,k} + \ell_3 \nu_k Q_{ik,j}.$$

By invoking the map Ψ, and mapping back to the reference domain Ω_{ref}, one can show that (14) has a unique solution by the standard theory of parabolic PDEs [18, 30].

2.4 Variational Formulation

The function space for posing the weak formulation of the time-dependent LdG problem is given by $\mathbf{Q} \equiv \mathbf{Q}(\Omega) := H^1(\Omega; \mathbf{S}_0)$, which is posed on $\Omega(t)$ for each $t \in [0, T]$. In case we impose Dirichlet conditions (strong anchoring) on $\partial\widehat{\mathfrak{D}}$, we define

$$\mathbf{Q}(\Omega) = \{P \in H^1(\Omega; \mathbf{S}_0) \mid P = R|_\Omega, \text{ for } R \in H^1_0(\widehat{\mathfrak{D}}; \mathbf{S}_0)\}.$$

Note that $\mathbf{S}_0$ can be uniquely identified with a five dimensional vector space [19], i.e. there exists 3×3, symmetric traceless basis matrices $\{E^i\}_{i=1}^5$ such that any $Q \in \mathbf{S}_0$ can be uniquely expressed as $Q = q_i E^i$, for some coefficients $q_1, \ldots, q_5$. Therefore, $\mathbf{Q}$ is isomorphic to $H^1(\Omega; \mathbb{R}^5)$. Moreover, we choose $\{E^i\}_{i=1}^5$ to be an orthonormal basis with respect to the Frobenius inner product. Upon setting $\mathbf{q} := (q_1, q_2, q_3, q_4, q_5)^\dagger$, we note the following properties [19]:

$$Q : P = \mathbf{q} \cdot \mathbf{p}, \qquad |Q|^2 = |\mathbf{q}|^2, \qquad |\nabla Q|^2 = |\nabla \mathbf{q}|^2. \tag{17}$$

2.4.1 Preliminaries

We summarize some basic results that are needed in the well-posedness of the weak formulation. The following theorem [15, Lem. 4.1] establishes this result for the ℓ_1, ℓ_2, ℓ_3 terms in the elastic energy. Throughout this subsection, we suppress time notation t.

Theorem 1. *Let $a_e(\Omega; \cdot, \cdot) : \mathbf{Q} \times \mathbf{Q} \to \mathbb{R}$ be the symmetric bilinear form defined by* (15)*. Then $a_e(\Omega; \cdot, \cdot)$ is bounded. If ℓ_1, ℓ_2, ℓ_3 satisfy*

$$0 < \ell_1, \quad -\ell_1 < \ell_3 < 2\ell_1, \quad -\frac{3}{5}\ell_1 - \frac{1}{10}\ell_3 < \ell_2, \tag{18}$$

then there is a constant $c > 0$ such that $a_e(\Omega; P, P) \geq c\|\nabla P\|^2_{0,\Omega}$ for all $P \in \mathbf{Q}$.

The next result can be found in [26, Prop. 5].

Proposition 1 (Coercivity)**.** *Let $a_s(\Omega; \cdot, \cdot) : \mathbf{Q} \times \mathbf{Q} \to \mathbb{R}$ be the symmetric bilinear form defined by*

$$a_s(\Omega; Q, P) = w_0 (Q, P)_\Gamma + w_1 \left(Q - Q^\perp, P\right)_\Gamma. \tag{19}$$

There exists a constant $\alpha_1 > 0$ such that

$$a_e(\Omega; P, P) + a_s(\Omega; P, P) \geq \alpha_1 \|P\|^2_{1,\Omega}, \qquad \forall P \in \mathbf{Q}. \tag{20}$$

We also have the bilinear form $a_{\mathrm{t}}(\Omega; \cdot, \cdot) : \mathbf{Q} \times \mathbf{Q} \to \mathbb{R}$ from (16), which is *not* coercive, that accounts for the twist term that satisfies the bound

$$a_{\mathrm{t}}(\Omega; Q, P) \leq 2\ell_1\tau_0\sqrt{27}\left[|Q|_{1,\Omega}\|P\|_{0,\Omega} + |P|_{1,\Omega}\|Q\|_{0,\Omega}\right]. \tag{21}$$

For later use, we define one bilinear form to contain (15), (19), and (16):

$$\tilde{a}(\Omega; Q, P) = a_{\mathrm{e}}(\Omega; Q, P) + a_{\mathrm{t}}(\Omega; Q, P) + a_{\mathrm{s}}(\Omega; Q, P), \tag{22}$$

which satisfies the following continuity result.

Proposition 2 (Continuity)**.** *There holds*

$$\begin{aligned} a_e(\Omega; Q, P) &\le c_e |Q|_{1,\Omega} |P|_{1,\Omega}, \quad a_t(\Omega; Q, P) \le c_t \|Q\|_{1,\Omega} \|P\|_{1,\Omega}, \\ a_s(\Omega; Q, P) &\le c_s \|Q\|_{0,\Gamma} \|P\|_{0,\Gamma}, \quad \tilde{a}(\Omega; Q, P) \le c_0 \|Q\|_{1,\Omega} \|P\|_{1,\Omega}, \end{aligned} \tag{23}$$

for all $Q, P \in \mathbf{Q}$*, where*

$$c_e = \ell_1 + 3\ell_2 + \ell_3, \ c_t = 2\sqrt{27}\ell_1\tau_0, \ c_s = w_0 + 3w_1, \ c_0 = c_e + c_t + \beta_3 c_s, \tag{24}$$

where $\beta_3 > 0$ *is a trace embedding constant depending on* Ω*.*

2.4.2 Weak Form

Using (22), we can now write $E[Q]$ in the form

$$\begin{aligned} E[Q] = &\frac{1}{2}\tilde{a}(\Omega; Q, Q) + \frac{1}{\eta^2}(\psi(Q), 1)_\Omega + \frac{1}{\omega}(\phi(Q), 1)_\Gamma - (\chi(Q), 1)_\Omega \\ &- w_0 (Q_\Gamma, Q)_\Gamma - w_1 \left(-\frac{s_0}{3}\boldsymbol{\nu}\otimes\boldsymbol{\nu}, Q\right)_\Gamma + \frac{w_0}{2}\|Q_\Gamma\|^2_{L^2(\Gamma)} + \frac{w_1}{2}\left(\frac{s_0}{3}\right)^2 \|\boldsymbol{\nu}\otimes\boldsymbol{\nu}\|^2_{L^2(\Gamma)}, \end{aligned} \tag{25}$$

which gives the first variation of E as:

$$\begin{aligned} \delta_Q E[Q; P] = &\tilde{a}(\Omega(t); Q, P) + (1/\eta^2)(\psi'(Q), P)_{\Omega(t)} + (1/\omega)(\phi'(Q), P)_{\Gamma(t)} \\ &- (\chi(P), 1)_{\Omega(t)} - w_0 (Q_\Gamma, P)_{\Gamma(t)} - w_1 \left(-\frac{s_0}{3}\boldsymbol{\nu}\otimes\boldsymbol{\nu}, P\right)_{\Gamma(t)}. \end{aligned} \tag{26}$$

Then, by (13), we have the weak form of (14):

$$(\partial_t Q, P)_{\Omega(t)} + ((\mathbf{v}\cdot\nabla)Q, P)_{\Omega(t)} + \delta_Q E[Q; P] = (B(\nabla\mathbf{v}, Q), P)_{\Omega(t)} + \frac{2p_0}{3}(S, P)_{\Omega(t)}, \ \forall P \in \mathbf{Q}(\Omega(t)), \tag{27}$$

for all $t \in [0, T]$. Next, for convenience, we define a right-hand-side linear form l_{rhs}:

$$l_{\mathrm{rhs}}(P) = (U_\Omega, P)_{\Omega(t)} + w_0 (Q_\Gamma, P)_{\Gamma(t)} + w_1 \left(-\frac{s_0}{3}\boldsymbol{\nu}\otimes\boldsymbol{\nu}, P\right)_{\Gamma(t)} + \frac{2p_0}{3}(S, P)_{\Omega(t)}. \tag{28}$$

Then, after invoking a modification of the advective term [34], we rewrite the weak form as follows. Find $Q(t,\cdot) \in \mathbf{Q}(\Omega(t))$ such that

$$\begin{aligned} &(\partial_t Q, P)_{\Omega(t)} + \frac{1}{2}((\mathbf{v}\cdot\nabla)Q, P)_{\Omega(t)} - \frac{1}{2}((\mathbf{v}\cdot\nabla)P, Q)_{\Omega(t)} + \frac{1}{2}((\boldsymbol{\nu}\cdot\mathbf{v})Q, P)_{\Gamma(t)} \\ &\quad + \tilde{a}(\Omega(t); Q, P) + \frac{1}{\eta^2}(\psi'(Q), P)_{\Omega(t)} + \frac{1}{\omega}(\phi'(Q), P)_{\Gamma(t)} - (B(\nabla\mathbf{v}, Q), P)_{\Omega(t)} \\ &\quad = l_{\mathrm{rhs}}(P), \qquad \forall P \in \mathbf{Q}(\Omega(t)), \end{aligned} \tag{29}$$

for a.e. $t \in [0, T]$, where $Q(0,\cdot) := Q_0(\cdot) \in \mathbf{Q}(\Omega(0))$.

For the analysis, we note that ψ and ϕ satisfy $\psi'(0) = \phi'(0) = 0$, and we make use of the following convex splitting:

$$\psi =: \psi_c - \psi_e, \quad \phi =: \phi_c - \phi_e, \tag{30}$$

where ψ_c, ψ_e, ϕ_c, and ϕ_e are all convex with ψ_e and ϕ_e quadratic, i.e.

$$\psi_e := \beta_\psi |Q|^2, \quad \text{with} \quad \beta_\psi = \frac{1}{4} + \frac{a_2}{2} + \frac{a_3^2}{4a_4}, \quad \phi_e := \beta_\phi |Q|^2, \tag{31}$$

where $\beta_\phi > 0$ is sufficiently large. Moreover, $\psi_c \ge 0$ and $\phi_c \ge 0$. Due to our specific ψ and ϕ, we note that ψ_c is quartic and has a similar form as (6) and that ϕ_c has quadratic growth like (9) and satisfies inequalities (10). More specifically, we have

$$\psi_c'(Q) : Q \ge \frac{1}{2}|Q|^2 + \frac{a_4}{2}|Q|^4. \tag{32}$$

This will be useful in some of the proofs in the following sections.

3 Time Semi-discrete Method

We first discretize in time the problem (29). We take a uniform time step given by $\triangle t := T/N$, where T is the final time and N is the number of time steps to be taken. Also, let $t_n := n\triangle t$ and denote $Q^n(\boldsymbol{x}) := Q(t_n, \boldsymbol{x})$ with analogous definitions for Ω^n, Γ^n, U^n_Ω, Q^n_Γ, $\mathbf{v}^n$, etc.

We need an extension operator in order to compare functions on domains at different times. If E is a domain, then let $\mathcal{O}_\delta(E) := \{\boldsymbol{x} \mid \mathrm{dist}(\boldsymbol{x}, E) < \delta\}$ be a slightly larger domain with extra thickness $\delta > 0$. We require that

$$\Omega^n \subset \mathcal{O}_\delta(\Omega^{n-1}), \quad \text{for } n = 1, ..., N, \tag{33}$$

which is guaranteed if

$$\delta = c_\delta \mathbf{v}^n_\infty \triangle t, \quad \mathbf{v}^n_\infty := \max_{t\in[0,T]} \|\mathbf{v}\cdot\boldsymbol{\nu}\|_{L^\infty(\Gamma(t))}, \quad c_\delta > 1. \tag{34}$$

The time-discrete version of (14) is given by replacing $\partial_t Q$ with

$$\frac{Q^n - \mathcal{E}Q^{n-1}}{\triangle t}.$$

Here, we use the implicit Euler method for the time derivative, which is well-defined because of the extension operator $\mathcal{E} : H^1(\Omega^{n-1}) \to H^1(\mathcal{O}_\delta(\Omega^{n-1}))$ (see Appendix A.1).

3.1 Variational Formulation

We begin by defining some convenient linear and bilinear forms:

$$\begin{aligned} a^n(Q,P) &= \tilde{a}(\Omega^n; Q, P) + \frac{1}{2}((\mathbf{v}\cdot\nabla)Q, P)_{\Omega^n} - \frac{1}{2}((\mathbf{v}\cdot\nabla)P, Q)_{\Omega^n} + \frac{1}{2}((\boldsymbol{\nu}\cdot\mathbf{v})Q, P)_{\Gamma^n}, \\ l^n_{\mathrm{rhs}}(P) &= (U^n_\Omega, P)_{\Omega^n} + w_0 (Q^n_\Gamma, P)_{\Gamma^n} + w_1 \left(-\frac{s_0}{3}\boldsymbol{\nu}\otimes\boldsymbol{\nu}, P\right)_{\Gamma^n} + \frac{2p_0}{3}(S,P)_{\Omega^n}, \end{aligned} \tag{35}$$

where $a^n(\cdot,\cdot)$ satisfies the following elementary coercivity result.

Proposition 3 (Gårding inequality)**.** *There holds*

$$a^n(P,P) \ge \frac{\alpha_1}{2}\|P\|^2_{H^1(\Omega^n)} - \theta_1 \|P\|^2_{L^2(\Omega^n)}, \tag{36}$$

for all $P \in \mathbf{Q}$, where $\theta_1 = \left(4\ell_1\tau_0\sqrt{27} + \frac{C_{\Gamma^n}}{2}\|\boldsymbol{\nu}\cdot\mathbf{v}\|_{L^\infty(\Gamma^n)}\right)^2/(2\alpha_1)$ and $C_{\Gamma^n} > 0$ is a trace embedding constant.

Proof. We start with

$$\begin{aligned} a^n(P,P) &= \tilde{a}(\Omega^n; P, P) + \frac{1}{2}((\boldsymbol{\nu}\cdot\mathbf{v})P, P)_{\Gamma^n} \\ &\ge \alpha_1\|P\|^2_{H^1(\Omega^n)} - 4\ell_1\tau_0\sqrt{27}\|\nabla P\|_{L^2(\Omega^n)}\|P\|_{L^2(\Omega^n)} - \frac{1}{2}\|\boldsymbol{\nu}\cdot\mathbf{v}\|_{L^\infty(\Gamma^n)}\|P\|^2_{L^2(\Gamma^n)} \\ &\ge \alpha_1\|P\|^2_{H^1(\Omega^n)} - \left(4\ell_1\tau_0\sqrt{27} + \frac{C_{\Gamma^n}}{2}\|\boldsymbol{\nu}\cdot\mathbf{v}\|_{L^\infty(\Gamma^n)}\right)\|P\|_{H^1(\Omega^n)}\|P\|_{L^2(\Omega^n)}, \end{aligned}$$

where we used a trace estimate. By a weighted Young inequality, we get (36). □

The weak formulation for the time semi-discrete version of (29) is as follows. For each $n = 1, 2, ...N$, find $Q^n \in \mathbf{Q}(\Omega^n)$ such that for all $P \in \mathbf{Q}(\Omega^n)$ we have

$$\begin{aligned} G^n(Q^n, P) := \frac{1}{\triangle t}(Q^n, P)_{\Omega^n} + a^n(Q^n, P) + \frac{1}{\eta^2}(\psi'(Q^n), P)_{\Omega^n} + \frac{1}{\omega}(\phi'(Q^n), P)_{\Gamma^n} \\ - (B(\nabla\mathbf{v}, Q^n), P)_{\Omega^n} = l^n_{\mathrm{rhs}}(P) + \frac{1}{\triangle t}\left(\mathcal{E}Q^{n-1}, P\right)_{\Omega^n} =: \Theta(P), \end{aligned} \tag{37}$$

where $Q^0 := Q_0$ is the initial state.

3.2 Solvability

We will establish the unique solvability of (37) for a sufficiently small time step. First, we derive a kind of Gårding inequality.

Lemma 1 (Lower bound)**.** *For all $Q \in \mathbf{Q}(\Omega^n)$, we have*

$$\begin{aligned} a^n(Q,Q) - (B(\nabla\mathbf{v},Q),Q)_{\Omega^n} + \frac{1}{\eta^2}(\psi'(Q),Q)_{\Omega^n} + \frac{1}{\omega}(\phi'(Q),Q)_{\Gamma^n} \\ \geq \frac{\alpha_1}{4}\|\nabla Q\|^2_{L^2(\Omega^n)} + \frac{a_4}{4\eta^2}\|Q\|^4_{L^4(\Omega^n)} - \zeta'\|Q\|^2_{L^2(\Omega^n)}, \end{aligned} \tag{38}$$

where $\zeta' = \left[\frac{C^2_{\Omega^n}\zeta_1^2}{\alpha_1} + \zeta_2 - \frac{3\alpha_1}{4} - \frac{1}{2\eta^2}\right]$ *and* $\zeta_1 = \frac{2\beta_\phi}{\omega} + \frac{1}{2}\|\mathbf{v}\cdot\boldsymbol{\nu}\|_{L^\infty(\Gamma^n)}$ *and* $\zeta_2 = \frac{216\ell_1^2\tau_0^2}{\alpha_1} + \frac{2\beta_\psi}{\eta^2} + 2\|\nabla\mathbf{v}\|_\infty + \frac{4\eta^2}{a_4}\|\nabla\mathbf{v}\|^2_\infty$*, where β_ψ and β_ϕ come from the convex splitting in* (31)*.*

Proof. We begin with

$$\begin{aligned} & a^n(Q,Q) - (B(\nabla\mathbf{v},Q),Q)_{\Omega^n} + \frac{1}{\eta^2}(\psi'(Q),Q)_{\Omega^n} + \frac{1}{\omega}(\phi'(Q),Q)_{\Gamma^n} \\ &= \tilde{a}(\Omega^n;Q,Q) - (B(\nabla\mathbf{v},Q),Q)_{\Omega^n} + \frac{1}{2}((\boldsymbol{\nu}\cdot\mathbf{v})Q,Q)_{\Gamma^n} + \frac{1}{\eta^2}(\psi'(Q),Q)_{\Omega^n} + \frac{1}{\omega}(\phi'(Q),Q)_{\Gamma^n} \\ &\geq \alpha_1\|Q\|^2_{H^1(\Omega^n)} + a_{\mathrm{t}}(\Omega^n;Q,Q) - (B(\nabla\mathbf{v},Q),Q)_{\Omega^n} - \frac{1}{2}\|\boldsymbol{\nu}\cdot\mathbf{v}\|_{L^\infty(\Gamma^n)}\|Q\|^2_{L^2(\Gamma^n)} \\ &\quad + \frac{1}{\eta^2}(\psi'(Q),Q)_{\Omega^n} + \frac{1}{\omega}(\phi'(Q),Q)_{\Gamma^n}, \end{aligned} \tag{39}$$

where we have used Proposition 1. We will also use equation (21) to handle the $a_{\mathrm{t}}(\Omega^n;Q,Q)$ term. Hence $a_{\mathrm{t}}(\Omega^n;Q,Q) \leq 4\ell_1\tau_0\sqrt{27}|Q|_{1,\Omega}\|Q\|_{0,\Omega}$. To deal with the Beris–Edwards term, we start with

$$\begin{aligned} -(B(\nabla\mathbf{v},Q),Q)_{\Omega^n} &= -2p_0\left(\nabla\mathbf{v},Q^2\right)_{\Omega^n} + 2p_0\int_{\Omega^n}(\nabla\mathbf{v}:Q)(Q:Q)d\boldsymbol{x} \\ &\geq -2p_0\|\nabla\mathbf{v}\|_\infty\|Q\|^2_{L^2(\Omega^n)} - 2p_0\|\nabla\mathbf{v}\|_\infty\int_{\Omega^n}|Q|^3d\boldsymbol{x}. \end{aligned} \tag{40}$$

Since $|p_0| \leq 1$, $\phi_c'(0) = 0$, $0 \leq [\phi_c'(Q) - \phi_c'(0)] : (Q - 0)$ (by convexity), and a weighted Young's inequality, we get

$$
\begin{aligned}
&a^n(Q,Q) - (B(\nabla\mathbf{v},Q),Q)_{\Omega^n} + \frac{1}{\eta^2}(\psi'(Q),Q)_{\Omega^n} + \frac{1}{\omega}(\phi'(Q),Q)_{\Gamma^n}\\
&\quad\geq \alpha_1\|Q\|^2_{H^1(\Omega^n)} - 4\ell_1\tau_0\sqrt{27}\|\nabla Q\|_{L^2(\Omega^n)}\|Q\|_{L^2(\Omega^n)} - \frac{1}{2}\|\boldsymbol{\nu}\cdot\mathbf{v}\|_{L^\infty(\Gamma^n)}\|Q\|^2_{L^2(\Gamma^n)} + \frac{1}{\eta^2}(\psi_c'(Q)-\psi_e'(Q),Q)_{\Omega^n}\\
&\qquad + \frac{1}{\omega}(\phi_c'(Q)-\phi_e'(Q),Q)_{\Gamma^n} - 2p_0\|\nabla\mathbf{v}\|_\infty\|Q\|^2_{L^2(\Omega^n)} - 2p_0\|\nabla\mathbf{v}\|_\infty\int_{\Omega^n}|Q|^3 d\boldsymbol{x}\\
&\geq \alpha_1\|Q\|^2_{H^1(\Omega^n)} - 4\ell_1\tau_0\sqrt{27}\|\nabla Q\|_{L^2(\Omega^n)}\|Q\|_{L^2(\Omega^n)} - \frac{1}{2}\|\boldsymbol{\nu}\cdot\mathbf{v}\|_{L^\infty(\Gamma^n)}\|Q\|^2_{L^2(\Gamma^n)} + \frac{1}{2\eta^2}\|Q\|^2_{L^2(\Omega^n)} + \frac{a_4}{2\eta^2}\|Q\|^4_{L^4(\Omega^n)}\\
&\quad - \frac{2\beta_\psi}{\eta^2}\|Q\|^2_{L^2(\Omega^n)} - \frac{2\beta_\phi}{\omega}\|Q\|^2_{L^2(\Gamma^n)} - 2p_0\|\nabla\mathbf{v}\|_\infty\|Q\|^2_{L^2(\Omega^n)} - 2p_0\|\nabla\mathbf{v}\|_\infty\int_{\Omega^n}|Q|^3 d\boldsymbol{x}\\
&\quad\geq \frac{\alpha_1}{2}\|\nabla Q\|^2_{L^2(\Omega^n)} + \alpha_1\|Q\|^2_{L^2(\Omega^n)} - \left[\frac{2\beta_\phi}{\omega} + \frac{1}{2}\|\boldsymbol{\nu}\cdot\mathbf{v}\|_{L^\infty(\Gamma^n)}\right]\|Q\|^2_{L^2(\Gamma^n)} + \frac{a_4}{4\eta^2}\|Q\|^4_{L^4(\Omega^n)}\\
&\qquad + \left[\frac{1}{2\eta^2} - \left(\frac{216\ell_1^2\tau_0^2}{\alpha_1} + \frac{2\beta_\psi}{\eta^2} + 2\|\nabla\mathbf{v}\|_\infty + \frac{4\eta^2}{a_4}\|\nabla\mathbf{v}\|^2_\infty\right)\right]\|Q\|^2_{L^2(\Omega^n)}\\
&\quad\geq \frac{\alpha_1}{2}\|\nabla Q\|^2_{L^2(\Omega^n)} - C_{\Omega^n}\zeta_1\|Q\|_{L^2(\Omega^n)}\|Q\|_{H^1(\Omega^n)} + \frac{a_4}{4\eta^2}\|Q\|^4_{L^4(\Omega^n)} + \left[\alpha_1 + \frac{1}{2\eta^2} - \zeta_2\right]\|Q\|^2_{L^2(\Omega^n)}\\
&\quad\geq \frac{\alpha_1}{2}\|\nabla Q\|^2_{L^2(\Omega^n)} - \frac{C^2_{\Omega^n}\zeta_1^2}{\alpha_1}\|Q\|^2_{L^2(\Omega^n)} - \frac{\alpha_1}{4}\|Q\|^2_{H^1(\Omega^n)} + \frac{a_4}{4\eta^2}\|Q\|^4_{L^4(\Omega^n)} + \left[\alpha_1 + \frac{1}{2\eta^2} - \zeta_2\right]\|Q\|^2_{L^2(\Omega^n)}\\
&\quad= \frac{\alpha_1}{4}\|\nabla Q\|^2_{L^2(\Omega^n)} + \frac{a_4}{4\eta^2}\|Q\|^4_{L^4(\Omega^n)} - \left[\frac{C^2_{\Omega^n}\zeta_1^2}{\alpha_1} + \zeta_2 - \frac{3\alpha_1}{4} - \frac{1}{2\eta^2}\right]\|Q\|^2_{L^2(\Omega^n)} =: A_0,
\end{aligned}
\tag{41}
$$

where $\zeta_1 = \frac{2\beta_\phi}{\omega} + \frac{1}{2}\|\boldsymbol{\nu}\cdot\mathbf{v}\|_{L^\infty(\Gamma^n)}$ and $\zeta_2 = \frac{216\ell_1^2\tau_0^2}{\alpha_1} + \frac{2\beta_\psi}{\eta^2} + 2\|\nabla\mathbf{v}\|_\infty + \frac{4\eta^2}{a_4}\|\nabla\mathbf{v}\|^2_\infty$, which gives the assertion. □

We establish the solvability of (37) using monotonicity methods. Note that we cannot use a minimization approach because $B(\nabla\mathbf{v}, Q^n)$ cannot be written as the variational derivative of some function.

Theorem 2. *For any $n = 1, ..., N$, and any $\triangle t > 0$, there exists a solution of* (37)*.*

Proof. We consider (37) at time step $n \in \{1, ..., N\}$. Let $\{P_k\}_{k=1}^\infty$ be an orthonormal basis of $\mathbf{Q}(\Omega^n)$ and make a finite dimensional approximation of Q^n:

$$
Q_m^n = \sum_{k=1}^m \gamma_{m,k}P_k, \tag{42}
$$

where $\gamma_{m,k}$ is chosen so that Q_m^n solves

$$
G^n(Q_m^n, P_k) = \Theta(P_k), \quad \text{for } k = 1, ..., m, \tag{43}
$$

where $1 \leq m < \infty$. We now show that for each $m = 1, 2, ...$, there exists Q_m^n of the form (42) that solves (43).

Define the continuous function $\boldsymbol{\omega} : \mathbb{R}^m \to \mathbb{R}^m$, with $\boldsymbol{\omega} = (\omega_1, ..., \omega_m)$ by

$$
\omega_k(\boldsymbol{\gamma}) := G^n\left(\sum_{j=1}^m \gamma_j P_j, P_k\right) - \Theta(P_k), \quad \text{for } k = 1, ..., m, \tag{44}
$$

where $\boldsymbol{\gamma} = (\gamma_1, ..., \gamma_m)$ and $Q = \sum_{j=1}^m \gamma_j P_j$. Then,

$$
\boldsymbol{\omega}(\boldsymbol{\gamma}) \cdot \boldsymbol{\gamma} = G^n(Q,Q) - \Theta(Q), \tag{45}
$$

and note that $|\Theta(Q)| \leq C_0 \|Q\|_{H^1(\Omega^n)} \leq C_0 |\boldsymbol{\gamma}|$ by the orthonormality of $\{P_k\}$. Thus, with the help of (37) and (38), we obtain

$$\begin{aligned} \boldsymbol{\omega}(\boldsymbol{\gamma}) \cdot \boldsymbol{\gamma} &\geq \frac{\alpha_1}{4} \|\nabla Q\|_{L^2(\Omega^n)}^2 + \frac{1}{\triangle t} \|Q\|_{L^2(\Omega^n)}^2 + \frac{a_4}{4\eta^2} \|Q\|_{L^4(\Omega^n)}^4 - \zeta' \|Q\|_{L^2(\Omega^n)}^2 - C_0 |\boldsymbol{\gamma}| \\ &\geq C_1 \|Q\|_{H^1(\Omega^n)}^2 - C_0 |\boldsymbol{\gamma}| + \int_{\Omega^n} \frac{a_4}{4\eta^2} |Q|^4 - \zeta' |Q|^2 d\boldsymbol{x}, \end{aligned} \tag{46}$$

for some constant $C_1 > 0$.

If $\zeta' > 0$, then set $\varpi_0 = \zeta' \eta a_4^{-1/2}$ and rewrite (46) by completing the square to get

$$\boldsymbol{\omega}(\boldsymbol{\gamma}) \cdot \boldsymbol{\gamma} \geq C_1 |\boldsymbol{\gamma}|^2 - C_0 |\boldsymbol{\gamma}| + \int_{\Omega^n} \left(\frac{a_4^{1/2}}{2\eta} |Q|^2 - \varpi_0 \right)^2 d\boldsymbol{x} - \varpi_0^2 |\Omega^n| \geq C_1 |\boldsymbol{\gamma}|^2 - C_0 |\boldsymbol{\gamma}| - \varpi_0^2 |\Omega^n|. \tag{47}$$

Clearly, $\boldsymbol{\omega}(\boldsymbol{\gamma}) \cdot \boldsymbol{\gamma} \geq 0$ if $|\boldsymbol{\gamma}| = r$ and r is sufficiently large. Hence, by [17, Sec. 9.1, Lemma], there exists a $\boldsymbol{\gamma}_m \in B(0, r)$ such that $\boldsymbol{\omega}(\boldsymbol{\gamma}_m) = \mathbf{0}$, i.e. there exists Q_m^n of the form (42) that solves (43).

Next, we need an a priori estimate. Multiply (43) by $\gamma_{m,k}$ and sum over k to get $G^n(Q_m^n, Q_m^n) = \Theta(Q_m^n)$, and using (38) gives

$$\frac{\alpha_1}{4} \|\nabla Q_m^n\|_{L^2(\Omega^n)}^2 + \frac{1}{\triangle t} \|Q_m^n\|_{L^2(\Omega^n)}^2 + \frac{a_4}{4\eta^2} \|Q_m^n\|_{L^4(\Omega^n)}^4 - \zeta' \|Q_m^n\|_{L^2(\Omega^n)}^2 \leq C_0 \|Q_m^n\|_{H^1(\Omega^n)}. \tag{48}$$

Using a weighted Young's inequality, one can show that

$$\|Q_m^n\|_{H^1(\Omega^n)}^2 - C_2 \leq C_3 \|Q_m^n\|_{H^1(\Omega^n)}, \tag{49}$$

for some positive constants C_2, C_3. Another weighted Young's inequality delivers $\|Q_m^n\|_{H^1(\Omega^n)} \leq C_4$ for some constant $C_4 > 0$ that is independent of m.

Therefore, $Q_m^n \rightharpoonup Q^n$ in $H^1(\Omega^n)$, which implies that $Q_m^n \to Q^n$ in $L^{6-\epsilon}(\Omega^n)$ for any $\epsilon > 0$. By standard arguments, one can show that Q^n satisfies (37). □

Corollary 1. *Assume* $\triangle t$ *satisfies* $0 < \triangle t < \max(\xi_0, 0)^{-1}$ *where*

$$\xi_0 := \left(\frac{\beta_\phi}{\omega} + \frac{1}{2} \|\boldsymbol{\nu} \cdot \mathbf{v}\|_{L^\infty(\Gamma^n)} \right)^2 \frac{C_{\Omega^n}^2}{\alpha_1} + \frac{3a_3^2}{2a_4\eta^2} + \frac{432\ell_1^2\tau_0^2}{\alpha_1} + \frac{\beta_\psi}{\eta^2} + \|\nabla \mathbf{v}\|_\infty + \frac{2\eta^2}{a_4} \|\nabla \mathbf{v}\|_\infty^2 - \frac{1}{2\eta^2} - \frac{\alpha_1}{2}. \tag{50}$$

Then, for any $n = 1, ..., N$*, there exists a* unique *solution of* (37).

Proof. We consider (37) at time step $n \in \{1, ..., N\}$. Assume that Q_1^n and Q_2^n are both solutions of (37). Subtracting the equations, we get

$$\begin{aligned} \frac{1}{\triangle t} \left(\bar{Q}^n, P \right)_{\Omega^n} + a^n \left(\bar{Q}^n, P \right) + \frac{1}{\eta^2} \left(\psi'(Q_1^n) - \psi'(Q_2^n), P \right)_{\Omega^n} + \frac{1}{\omega} \left(\phi'(Q_1^n) - \phi'(Q_2^n), P \right)_{\Gamma^n} \\ - \left(B(\nabla \mathbf{v}, Q_1^n) - B(\nabla \mathbf{v}, Q_2^n), P \right)_{\Omega^n} = 0, \quad \forall P \in \mathbf{Q}(\Omega^n), \end{aligned} \tag{51}$$

where we set $\bar{Q}^n := Q_1^n - Q_2^n$. We also note the identities:

$$\begin{aligned} [\psi_c'(Q_1^n) - \psi_c'(Q_2^n)] : P &= \left(\frac{1}{2} + \frac{a_3^2}{2a_4} \right) \bar{Q}^n : P - a_3 (\bar{Q}^n (Q_1^n + Q_2^n)) : P \\ &\quad + \frac{a_4}{2} \left[(|Q_1^n|^2 + |Q_2^n|^2) \bar{Q}^n : P + (\bar{Q}^n : (Q_1^n + Q_2^n))(P : (Q_1^n + Q_2^n)) \right], \\ B(\nabla \mathbf{v}, Q_1^n) - B(\nabla \mathbf{v}, Q_2^n) &= W \bar{Q}^n - \bar{Q}^n W + p_0 \left(\bar{Q}^n S + S \bar{Q}^n \right) \\ &\quad - 2p_0 (S : \bar{Q}^n) (Q_2^n + I/3) - 2p_0 (S : Q_1^n) \bar{Q}^n. \end{aligned} \tag{52}$$

Now, we estimate

$$\begin{aligned} T_0 :=& \frac{1}{\eta^2} [\psi_c'(Q_1^n) - \psi_c'(Q_2^n)] : \bar{Q}^n - \left(B(\nabla \mathbf{v}, Q_1^n) - B(\nabla \mathbf{v}, Q_2^n) \right) : \bar{Q}^n \\ =& \frac{1}{\eta^2} \left(\frac{1}{2} + \frac{a_3^2}{2a_4} \right) |\bar{Q}^n|^2 - \frac{a_3}{\eta^2} (\bar{Q}^n (Q_1^n + Q_2^n)) : \bar{Q}^n + \frac{a_4}{2\eta^2} \left[(|Q_1^n|^2 + |Q_2^n|^2) |\bar{Q}^n|^2 + |\bar{Q}^n : (Q_1^n + Q_2^n)|^2 \right] \\ &- \left(2p_0 \left(\bar{Q}^n S \right) : \bar{Q}^n \right) + 2p_0 (S : \bar{Q}^n) \left(Q_2^n : \bar{Q}^n \right) + 2p_0 (S : Q_1^n) |\bar{Q}^n|^2. \end{aligned} \tag{53}$$

Then, using weighted Young's inequalities,

$$
\begin{aligned}
T_0 &\geq \frac{1}{\eta^2}\left(\frac{1}{2}+\frac{a_3^2}{2a_4}-\frac{2a_3^2}{a_4}\right)|\bar{Q}^n|^2+\frac{a_4}{4\eta^2}(|Q_1^n|^2+|Q_2^n|^2)|\bar{Q}^n|^2 \\
&\quad -|\nabla\mathbf{v}||\bar{Q}^n|^2-|\nabla\mathbf{v}||\bar{Q}^n||Q_2^n||\bar{Q}^n|-|\nabla\mathbf{v}||\bar{Q}^n||Q_1^n||\bar{Q}^n| \\
&\geq \frac{1}{\eta^2}\left(\frac{1}{2}+\frac{a_3^2}{2a_4}-\frac{2a_3^2}{a_4}\right)|\bar{Q}^n|^2+\frac{a_4}{4\eta^2}(|Q_1^n|^2+|Q_2^n|^2)|\bar{Q}^n|^2 \\
&\quad -|\nabla\mathbf{v}||\bar{Q}^n|^2-\epsilon|\nabla\mathbf{v}|^2|\bar{Q}^n|^2-\frac{1}{2\epsilon}\left(|Q_1^n|^2+|Q_2^n|^2\right)|\bar{Q}^n|^2,
\end{aligned}
\tag{54}
$$

where $\epsilon > 0$ is chosen to be $\epsilon = 2\eta^2/a_4$. Thus, we get

$$
T_0 \geq \left[\frac{1}{\eta^2}\left(\frac{1}{2}+\frac{a_3^2}{2a_4}-\frac{2a_3^2}{a_4}\right)-|\nabla\mathbf{v}|-\frac{2\eta^2}{a_4}|\nabla\mathbf{v}|^2\right]|\bar{Q}^n|^2. \tag{55}
$$

Now, setting $P = \bar{Q}^n$ in (51) and using the convex splitting, we find that

$$
\begin{aligned}
&\frac{1}{\triangle t}\|\bar{Q}^n\|^2_{L^2(\Omega^n)}+a^n\left(\bar{Q}^n,\bar{Q}^n\right)-\frac{1}{\eta^2}\left(\psi_e'(Q_1^n)-\psi_e'(Q_2^n),\bar{Q}^n\right)_{\Omega^n}-\frac{1}{\omega}\left(\phi_e'(Q_1^n)-\phi_e'(Q_2^n),\bar{Q}^n\right)_{\Gamma^n} \\
&\qquad +\frac{1}{\eta^2}\left(\psi_c'(Q_1^n)-\psi_c'(Q_2^n),\bar{Q}^n\right)_{\Omega^n}-\left(B\left(\nabla\mathbf{v},Q_1^n\right)-B\left(\nabla\mathbf{v},Q_2^n\right),\bar{Q}^n\right)_{\Omega^n} \\
&\qquad +\frac{1}{\omega}\left(\phi_c'(Q_1^n)-\phi_c'(Q_2^n),\bar{Q}^n\right)_{\Gamma^n}=0,
\end{aligned}
\tag{56}
$$

and combining with (55) yields

$$
\begin{aligned}
&\frac{1}{\triangle t}\|\bar{Q}^n\|^2_{L^2(\Omega^n)}+a^n\left(\bar{Q}^n,\bar{Q}^n\right)-\frac{\beta_\phi}{\omega}\|\bar{Q}^n\|^2_{L^2(\Gamma^n)} \\
&\qquad +\left[\frac{1}{\eta^2}\left(\frac{1}{2}+\frac{a_3^2}{2a_4}-\frac{2a_3^2}{a_4}-\beta_\psi\right)-|\nabla\mathbf{v}|-\frac{2\eta^2}{a_4}|\nabla\mathbf{v}|^2\right]\|\bar{Q}^n\|^2_{L^2(\Omega^n)}\leq 0.
\end{aligned}
\tag{57}
$$

Next, we use coercivity and a trace estimate:

$$
\begin{aligned}
&\frac{1}{\triangle t}\|\bar{Q}^n\|^2_{L^2(\Omega^n)}+\alpha_1\|\bar{Q}^n\|^2_{H^1(\Omega^n)}-4\ell_1\tau_0\sqrt{27}\|\nabla\bar{Q}^n\|_{L^2(\Omega^n)}\|\bar{Q}^n\|_{L^2(\Omega^n)} \\
&\quad -\left(\frac{\beta_\phi}{\omega}+\frac{1}{2}\|\boldsymbol{\nu}\cdot\mathbf{v}\|_{L^\infty(\Gamma^n)}\right)C_{\Omega^n}\|\bar{Q}^n\|_{L^2(\Omega^n)}\|\bar{Q}^n\|_{H^1(\Omega^n)} \\
&\quad -\left[\frac{2a_3^2}{a_4\eta^2}+\frac{\beta_\psi}{\eta^2}+\|\nabla\mathbf{v}\|_\infty+\frac{2\eta^2}{a_4}\|\nabla\mathbf{v}\|^2_\infty-\frac{1}{\eta^2}\left(\frac{1}{2}+\frac{a_3^2}{2a_4}\right)\right]\|\bar{Q}^n\|^2_{L^2(\Omega^n)}\leq 0.
\end{aligned}
\tag{58}
$$

Again, using weighted Young's inequalities, we get

$$
\begin{aligned}
&\left[-\frac{432\ell_1^2\tau_0^2}{\alpha_1}-\left(\frac{\beta_\phi}{\omega}-\frac{1}{2}\|\boldsymbol{\nu}\cdot\mathbf{v}\|_{L^\infty(\Gamma^n)}\right)^2\frac{C_{\Omega^n}^2}{\alpha_1}\right. \\
&\quad \left.-\frac{3a_3^2}{2a_4\eta^2}-\frac{\beta_\psi}{\eta^2}-\|\nabla\mathbf{v}\|_\infty-\frac{2\eta^2}{a_4}\|\nabla\mathbf{v}\|^2_\infty+\frac{1}{2\eta^2}+\frac{\alpha_1}{2}+\frac{1}{\triangle t}\right]\|\bar{Q}^n\|^2_{L^2(\Omega^n)}\leq 0.
\end{aligned}
\tag{59}
$$

If $0 < \triangle t < \max(\xi_0, 0)^{-1}$, where ξ_0 is given by (50), then the left-hand-side bracket in (59) will be positive, which implies that $\bar{Q}^n = 0$, so then $Q_1^n = Q_2^n$. □

3.3 Stability of the Semi-discrete Method

Using the lower bound in Lemma 1, we derive a stability estimate that is *not* exponential in the final time T.

Lemma 2. *Let Q^n solve (37) for $n = 1, 2, ...N$. Then, we have the following stability estimate:*

$$(1 + C_2 \triangle t)\|Q^k\|^2_{L^2(\Omega^k)} + \frac{\alpha_1}{8} \triangle t \sum_{n=1}^{k} \|Q^n\|^2_{H^1(\Omega^n)} \leq C_1 \|Q^0\|^2_{L^2(\Omega^0)} + D, \text{ for all } k = 1, ..., N, \tag{60}$$

where $D = \triangle t \sum_{n=1}^{N} \left[\|U^n_\Omega\|^2_{L^2(\Omega^n)} + w_0^2 \|Q^n_\Gamma\|^2_{L^2(\Gamma^n)} + \frac{w_1^2 s_0^2}{9} |\Gamma^n|^2 + \frac{4p_0^2}{9} \|S\|^2_{L^2(\Omega^n)} + \frac{\eta^2}{2a_4} \kappa_0^2 |\Omega^n| \right]$ *with* $\zeta'' = \left[2\zeta' + \frac{4C^2_{\Omega^n}}{\alpha_1} + \frac{\alpha_1}{4} + 2 \right]$, $\kappa_0 = \max(0, \zeta'' + C_2 + \alpha_1/4)$, *and* C_1, C_2 *are constants that depend on the estimates of the extension operator.*

Proof. Recall (37)

$$\begin{aligned} \int_{\Omega^n} \frac{1}{\triangle t} Q^n : P d\boldsymbol{x} + a^n (Q^n, P) + \frac{1}{\eta^2} (\psi'(Q^n), P)_{\Omega^n} + \frac{1}{\omega} (\phi'(Q^n), P)_{\Gamma^n} - (B(\nabla \mathbf{v}, Q^n), P)_{\Omega^n} \\ = l^n_{\text{rhs}}(P) + \int_{\Omega^n} \frac{1}{\triangle t} Q^{n-1} : P d\boldsymbol{x}, \end{aligned} \tag{61}$$

and choose $P = 2\triangle t Q^n$ so that we get

$$\begin{aligned} 2\|Q^n\|^2_{L^2(\Omega^n)} + 2\triangle t a^n (Q^n, Q^n) + \frac{2\triangle t}{\eta^2} (\psi'(Q^n), Q^n)_{\Omega^n} + \frac{2\triangle t}{\omega} (\phi'(Q^n), Q^n)_{\Gamma^n} - 2\triangle t (B(\nabla \mathbf{v}, Q^n), Q^n)_{\Omega^n} \\ = 2\triangle t l^n_{\text{rhs}}(Q^n) + 2 \int_{\Omega^n} Q^{n-1} : Q^n d\boldsymbol{x}. \end{aligned} \tag{62}$$

And now, rearranging terms and applying Lemma 1, we obtain the following:

$$(1 - 2\triangle t \zeta')\|Q^n\|^2_{L^2(\Omega^n)} + \triangle t \frac{a_4}{2\eta^2} \|Q^n\|^4_{L^4(\Omega^n)} + \frac{\alpha_1}{2} \triangle t \|\nabla Q^n\|^2_{L^2(\Omega^n)} \leq 2\triangle t l^n_{\text{rhs}}(Q^n) + \|Q^{n-1}\|^2_{L^2(\Omega^n)}, \tag{63}$$

where we estimate $l^n_{\text{rhs}}(Q^n)$ as follows:

$$\begin{aligned} l^n_{\text{rhs}}(Q^n) &= (\chi^n(Q^n), 1)_{\Omega^n} + w_0 (Q^n_\Gamma, Q^n)_{\Gamma^n} + w_1 \left(-\frac{s_0}{3} \boldsymbol{\nu} \otimes \boldsymbol{\nu}, Q^n \right)_{\Gamma^n} + \frac{2p_0}{3} (S, Q^n)_{\Omega^n} \\ &= (U^n_\Omega, Q^n)_{\Omega^n} + w_0 (Q^n_\Gamma, Q^n)_{\Gamma^n} + w_1 \left(-\frac{s_0}{3} \boldsymbol{\nu} \otimes \boldsymbol{\nu}, Q^n \right)_{\Gamma^n} + \frac{2p_0}{3} (S, Q^n)_{\Omega^n} \\ &\leq \frac{1}{2} \|U^n_\Omega\|^2_{L^2(\Omega^n)} + \frac{w_0^2}{2} \|Q^n_\Gamma\|^2_{L^2(\Gamma^n)} + \frac{w_1^2 s_0^2}{18} \|\boldsymbol{\nu} \otimes \boldsymbol{\nu}\|^2_{L^2(\Gamma^n)} + \frac{2p_0^2}{9} \|S\|^2_{L^2(\Omega^n)} + \|Q^n\|^2_{L^2(\Omega^n)} + \|Q^n\|^2_{L^2(\Gamma^n)} \\ &\leq \frac{1}{2} \|U^n_\Omega\|^2_{L^2(\Omega^n)} + \frac{w_0^2}{2} \|Q^n_\Gamma\|^2_{L^2(\Gamma^n)} + \frac{w_1^2 s_0^2}{18} |\Gamma^n|^2 + \frac{2p_0^2}{9} \|S\|^2_{L^2(\Omega^n)} + \|Q^n\|^2_{L^2(\Omega^n)} + C_{\Omega^n} \|Q^n\|_{L^2(\Omega^n)} \|Q^n\|_{H^1(\Omega^n)} \\ &\leq \frac{1}{2} \|U^n_\Omega\|^2_{L^2(\Omega^n)} + \frac{w_0^2}{2} \|Q^n_\Gamma\|^2_{L^2(\Gamma^n)} + \frac{w_1^2 s_0^2}{18} |\Gamma^n|^2 + \frac{2p_0^2}{9} \|S\|^2_{L^2(\Omega^n)} \\ &\quad + \left[\frac{2C^2_{\Omega^n}}{\alpha_1} + \frac{\alpha_1}{8} + 1 \right] \|Q^n\|^2_{L^2(\Omega^n)} + \frac{\alpha_1}{8} \|\nabla Q^n\|^2_{L^2(\Omega^n)}. \end{aligned} \tag{64}$$

So then, by combining (63) and the above estimate, we get

$$(1 - \triangle t \zeta'') \|Q^n\|^2_{L^2(\Omega^n)} + \triangle t \frac{a_4}{2\eta^2} \|Q^n\|^4_{L^4(\Omega^n)} + \frac{\alpha_1}{4} \triangle t \|\nabla Q^n\|^2_{L^2(\Omega^n)} \leq \triangle t D^n + \|Q^{n-1}\|^2_{L^2(\Omega^n)}, \tag{65}$$

where $D^n = \|U^n_\Omega\|^2_{L^2(\Omega^n)} + w_0^2 \|Q^n_\Gamma\|^2_{L^2(\Gamma^n)} + \frac{w_1^2 s_0^2}{9} |\Gamma^n|^2 + \frac{4p_0^2}{9} \|S\|^2_{L^2(\Omega^n)}$ is part of the initial data and that $\zeta'' = \left[2\zeta' + \frac{4C^2_{\Omega^n}}{\alpha_1} + \frac{\alpha_1}{4} + 2 \right]$. Now using Lemmas 3.4 and 3.5 from [34], we get the following estimates for $\|Q^{n-1}\|^2_{L^2(\Omega^n)}$:

$$\begin{aligned} \|Q^0\|^2_{L^2(\Omega^1)} &\leq \|Q^0\|^2_{L^2(\mathcal{O}_\delta(\Omega^0))} \leq C_1 \|Q^0\|^2_{L^2(\Omega^0)}, \\ \|Q^{n-1}\|^2_{L^2(\Omega^n)} &\leq \|Q^{n-1}\|^2_{L^2(\mathcal{O}_\delta(\Omega^{n-1}))} \leq (1 + C_2 \triangle t) \|Q^{n-1}\|^2_{L^2(\Omega^{n-1})} + \frac{\alpha_1}{8} \triangle t \|\nabla Q^{n-1}\|^2_{L^2(\Omega^{n-1})}. \end{aligned} \tag{66}$$

Applying (66) to (65):

$$
\begin{aligned}
(1 - \triangle t\zeta'')\|Q^n\|^2_{L^2(\Omega^n)} &+ \triangle t\frac{a_4}{2\eta^2}\|Q^n\|^4_{L^4(\Omega^n)} + \frac{\alpha_1}{4}\triangle t\|\nabla Q^n\|^2_{L^2(\Omega^n)} \\
&\leq \triangle t D^n + C_1\|Q^{n-1}\|^2_{L^2(\Omega^{n-1})}, \text{ for } n = 1, \\
&\leq \triangle t D^n + (1 + C_2\triangle t)\|Q^{n-1}\|^2_{L^2(\Omega^{n-1})} + \frac{\alpha_1}{8}\triangle t\|\nabla Q^{n-1}\|^2_{L^2(\Omega^{n-1})}, \text{ for } n = 2, ..., k.
\end{aligned} \tag{67}
$$

Next, we take advantage of the quartic term $\|Q^n\|^4_{L^4(\Omega^n)}$. First, note the trivial inequality: $2\epsilon\|Q^n\|^2_{L^2(\Omega^n)} \leq \|Q^n\|^4_{L^4(\Omega^n)} + \epsilon^2|\Omega^n|$ for some $\epsilon > 0$. Then,

$$
\begin{aligned}
\frac{a_4}{2\eta^2}\|Q^n\|^4_{L^4(\Omega^n)} - \zeta''\|Q^n\|^2_{L^2(\Omega^n)} &\geq \left(\frac{a_4}{\eta^2}\epsilon - \zeta''\right)\|Q\|^2_{L^2(\Omega^n)} - \frac{a_4}{2\eta^2}\epsilon^2|\Omega^n| \\
&= \left(\frac{\alpha_1}{4} + C_2\right)\|Q\|^2_{L^2(\Omega^n)} - \frac{\eta^2}{2a_4}\kappa_0^2|\Omega^n|,
\end{aligned} \tag{68}
$$

by choosing $\epsilon = \eta^2 a_4^{-1}\kappa_0$, with $\kappa_0 = \max(0, \zeta'' + C_2 + \alpha_1/4)$. Combine this with (67) to get

$$
\begin{aligned}
(1 + C_2\triangle t)\|Q^n\|^2_{L^2(\Omega^n)} &- \triangle t\frac{\eta^2}{2a_4}\kappa_0^2|\Omega^n| + \frac{\alpha_1}{4}\triangle t\|Q^n\|^2_{H^1(\Omega^n)} \\
&\leq \triangle t D^n + C_1\|Q^{n-1}\|^2_{L^2(\Omega^{n-1})}, \text{ for } n = 1, \\
&\leq \triangle t D^n + (1 + C_2\triangle t)\|Q^{n-1}\|^2_{L^2(\Omega^{n-1})} + \frac{\alpha_1}{8}\triangle t\|\nabla Q^{n-1}\|^2_{L^2(\Omega^{n-1})}, \text{ for } n = 2, ..., k.
\end{aligned} \tag{69}
$$

Now, sum up (69) over $n = 1, ..., k$, and make some cancellation to obtain

$$
(1 + C_2\triangle t)\|Q^k\|^2_{L^2(\Omega^k)} + \frac{\alpha_1}{8}\triangle t\sum_{n=1}^{k}\|Q^n\|^2_{H^1(\Omega^n)} \leq C_1\|Q^0\|^2_{L^2(\Omega^0)} + \triangle t\left[\sum_{n=1}^{k} D^n + \frac{\eta^2}{2a_4}\kappa_0^2\sum_{n=1}^{k}|\Omega^n|\right]. \tag{70}
$$

□

4 Discretization in Time and Space

4.1 Preliminaries

4.1.1 Level Set Functions

The time-dependent domain $\Omega(t)$ is contained in an open "hold-all" domain $\widehat{\mathfrak{D}} \subset \mathbb{R}^d$ for all t. For convenience, we use a level set function $\phi : [0, T] \times \widehat{\mathfrak{D}} \to \mathbb{R}$ (at least C^2) to represent the exact domain $\Omega(t) = \{\boldsymbol{x} \in \widehat{\mathfrak{D}} : \phi(t, \boldsymbol{x}) < 0\}$. The boundary of $\Omega(t)$ partitions as $\partial\Omega(t) \equiv \Gamma(t) = \partial\widehat{\mathfrak{D}} \cup \widetilde{\Gamma}(t)$, where $\widetilde{\Gamma}(t) := \{\boldsymbol{x} \in \widehat{\mathfrak{D}} : \phi(t, \boldsymbol{x}) = 0\}$ is compactly contained in $\widehat{\mathfrak{D}}$ for all t (see Figure 1). To ensure $\widetilde{\Gamma}(t)$ is well-defined, we assume that $c^{-1} \geq |\nabla\phi(t, \boldsymbol{x})| \geq c > 0$, for all $t \in [0, T]$ in a neighborhood of $\widetilde{\Gamma}(t)$, for some constant c [43, 44].

The discrete domain is represented by a discrete version of ϕ, denoted ϕ_h. To this end, let $\widehat{\mathcal{T}}_h = \{T\}$ be a conforming shape regular mesh of $\widehat{\mathfrak{D}}$, where all $T \in \widehat{\mathcal{T}}_h$ are treated as open sets, and define the background (Lagrange) finite element space

$$
B_h^k = \{v_h \in C^0(\widehat{\mathfrak{D}}) : v_h|_T \in \mathcal{P}_k(T), \ \forall T \in \widehat{\mathcal{T}}_h\}, \ \ \text{for some } k \geq 1. \tag{71}
$$

Then, for some fixed $q \geq 1$, we let $\phi_h(t, \cdot) \in B_h^q$, for all t, and define the discrete domain $\Omega_h(t) = \{\boldsymbol{x} \in \widehat{\mathfrak{D}} : \phi_h(t, \boldsymbol{x}) < 0\}$ with $\partial\Omega_h(t) \equiv \Gamma_h(t) = \partial\widehat{\mathfrak{D}} \cup \widetilde{\Gamma}_h(t)$, where $\widetilde{\Gamma}_h(t) := \{\boldsymbol{x} \in \widehat{\mathfrak{D}} : \phi_h(t, \boldsymbol{x}) = 0\}$. Again, we assume $c^{-1} \geq |\nabla\phi_h| \geq c > 0$ a.e. in a neighborhood of $\widetilde{\Gamma}_h(t)$ to guarantee Ω_h is well-defined and $\widetilde{\Gamma}_h(t)$ has dimension $d - 1$.

4.1.2 Subdomains and Meshes

At each time step, we extend the discrete domain $\Omega_h^n = \Omega_h(t_n)$ to a larger set, denoted $\mathcal{O}_{\delta_h}(\Omega_h^n)$, where $\delta_h = c_{\delta_h} \mathbf{v}_\infty^n \triangle t$ with $c_\delta > c_{\delta_h} > 1$ specified later. With this, we define the active mesh and corresponding domain [44]:

$$\mathcal{T}_{\delta_h}^n \equiv \mathcal{T}_{\delta_h}(\Omega_h^n) = \{T \in \widehat{\mathcal{T}}_h : \mathcal{O}_{\delta_h}(\Omega_h^n) \cap T \neq \emptyset\}, \quad \mathfrak{D}_{\delta_h}^n \equiv \mathfrak{D}_{\delta_h}(\Omega_h^n) = \{\boldsymbol{x} \in T : T \in \mathcal{T}_{\delta_h}(\Omega_h^n)\}, \tag{72}$$

where the discrete extended domains $\mathfrak{D}_{\delta_h}^n$ are jagged versions of $\mathcal{O}_{\delta_h}(\Omega_h^n)$. Furthermore, we demand that $\delta > 0$ is sufficiently large so that

$$\mathfrak{D}_{\delta_h}^n \subset \mathcal{O}_\delta(\Omega^n), \quad \text{and} \quad \Omega_h^n \subset \mathcal{O}_\delta(\Omega(t)),\ t \in [t_{n-1}, t_n), \quad \text{for } n = 1, ..., N, \tag{73}$$

and we require that c_{δ_h} is sufficiently large so that the following containment holds:

$$\Omega_h^n \subset \mathfrak{D}_{\delta_h}^{n-1}, \quad \text{for } n = 1, ..., N, \tag{74}$$

which is a discrete version of (33).

Next, we define the tubular (or shell region) that contains $\widetilde{\Gamma}_h^n$:

$$\Sigma_{\delta_h}^n \equiv \Sigma_{\delta_h}(\widetilde{\Gamma}_h^n) = \{\boldsymbol{x} \in \widehat{\mathfrak{D}} : \text{dist}\left(\boldsymbol{x}, \widetilde{\Gamma}_h^n\right) \leq \delta_h\}, \tag{75}$$

i.e. the shell region always contains the zero level set. The corresponding mesh is

$$\mathcal{T}_{\Sigma_{\delta_h}}^n \equiv \mathcal{T}_{\Sigma_{\delta_h}}(\widetilde{\Gamma}_h^n) = \{T \in \widehat{\mathcal{T}}_h : T \cap \Sigma_{\delta_h}^n \neq \emptyset\}, \tag{76}$$

and we also have the set of shell facets:

$$\mathcal{F}_{\Sigma_{\delta_h}}^n = \{F \in \partial\mathcal{T}_{\delta_h}^n : F = \overline{T_1} \cap \overline{T_2},\ \text{for some } T_1 \in \mathcal{T}_{\delta_h}^n, T_2 \in \mathcal{T}_{\Sigma_{\delta_h}}^n,\ \text{such that } T_1 \neq T_2\}, \tag{77}$$

where $\partial\mathcal{T}_{\delta_h}^n := \{\partial T : T \in \mathcal{T}_{\delta_h}^n\}$ denotes the set of all facets within the active mesh. Note that the facets on the boundary of $\mathfrak{D}_{h,\delta}$ are *not* included in (77).

4.2 The Unfitted Finite Element Scheme

Let $\Omega_h^n = \Omega_h(t_n)$ be the discrete domain at time index t_n, i.e. $\Omega_h^n = \{\boldsymbol{x} \in \widehat{\mathfrak{D}} : \phi_h(t_n, \boldsymbol{x}) < 0\}$; we use similar superscript n notation for other quantities. We let $\mathbb{M}_h(\Omega_{h,\delta})$ be the space of continuous, piecewise Lagrange polynomial functions on $\Omega_{h,\delta}$, subordinate to the mesh $\mathcal{T}_{h,\delta}$ of $\Omega_{h,\delta}$, with polynomial degree $m \geq 1$, i.e.:

$$\mathbb{M}_h(\Omega_{h,\delta}) := \left\{v \in C^0(\mathfrak{D}_{h,\delta}) : v_h = \hat{v}_h|_{\mathfrak{D}_{h,\delta}},\ \text{for some } \hat{v}_h \in B_h^m|_{\mathfrak{D}_{h,\delta}}\right\}, \tag{78}$$

We discretize (14) by approximating Q by a finite element function Q_h. To this end, define

$$\mathbb{S}_h(\Omega_{h,\delta}) := \left\{P \in C^0(\mathfrak{D}_{h,\delta}; \mathbf{S}_0) \mid P = q_{i,h} E^i,\ q_{i,h} \in \mathbb{M}_h(\Omega_{h,\delta}), 1 \leq i \leq 5\right\}, \tag{79}$$

and let $Q_h \in \mathbf{Q}_h(\Omega_{h,\delta}) := \mathbb{S}_h(\Omega_{h,\delta})$. Thus, $Q_h = q_{i,h} E^i$, and $q_{i,h} \in H^1(\Omega)$ for $i = 1, \ldots, 5$.

The unfitted approach requires a special facet stabilization term in order to ensure a well-conditioned linear system to solve at each time step [9, 11, 10]. We define $s_h(\mathcal{F}; q, p)$, for $q, p \in \mathbb{M}_h(\Omega_{h,\delta})$, to be the global stabilization form given in [34, eqn. (4.8)], and extend this to $s_h(\mathcal{F}; Q, P)$, for $Q, P \in \mathbb{S}_h(\Omega_{h,\delta})$, using the basis matrices $\{E^i\}$. We will often make the abbreviation $s_h^n(\cdot,\cdot) := s_h\left(\mathcal{F}_{\Sigma_{\delta_h}}^n; \cdot, \cdot\right)$.

The facet stabilization requires a multiplicative constant factor, γ_s, that is based on properties of the underlying background mesh. To this end, we adopt [34, Assumption 5.3] and let $K \lesssim (1 + \delta_h/h)$ be the constant described there. Then, we set $\gamma_s = c_\gamma K$, where $c_\gamma > 0$ is independent of h and $\triangle t$. The following lemma is a summary of Lemmas 5.5 and 5.7 from [34].

Lemma 3. *Under [34, Assumption 5.3], there holds for* $v_h \in \mathbb{M}_h(\Omega_{h,\delta})$*:*

$$\begin{aligned} \|v_h\|^2_{\mathcal{O}_{\delta_h}(\Omega_h^n)} &\leq \|v_h\|^2_{\mathfrak{D}^n_{\delta_h}} \lesssim \|v_h\|^2_{\Omega_h^n} + Kh^2 s_h^n(v_h, v_h), \\ \|\nabla v_h\|^2_{\mathcal{O}_{\delta_h}(\Omega_h^n)} &\leq \|\nabla v_h\|^2_{\mathfrak{D}^n_{\delta_h}} \lesssim \|\nabla v_h\|^2_{\Omega_h^n} + K s_h^n(v_h, v_h), \end{aligned} \tag{80}$$

and for any $\epsilon > 0$*, we also have*

$$\|v_h\|^2_{\mathcal{O}_{\delta_h}(\Omega_h^n)} \leq (1 + C_a(\epsilon)\triangle t)\|v_h\|^2_{\Omega_h^n} + C_b(\epsilon)\alpha_1 \triangle t \|\nabla v_h\|^2_{\Omega_h^n} + C_c(\epsilon, h)\triangle t K s_h^n(v_h, v_h), \tag{81}$$

where

$$C_a(\epsilon) := c_L c_{\delta_h} \mathbf{v}^n_\infty (1 + \epsilon^{-1}), \quad C_b(\epsilon) := c_L c_{\delta_h} \mathbf{v}^n_\infty \epsilon/\alpha_1, \quad C_c(\epsilon, h) := c_L c_{\delta_h} \mathbf{v}^n_\infty (\epsilon + h^2 + h^2\epsilon^{-1}),$$

for some independent constant c_L*.*

Next, we define our discrete bilinear and linear forms:

$$\begin{aligned} a_h^n(Q_h, P_h) &= \tilde{a}(\Omega_h^n; Q_h, P_h) + \frac{1}{2}((\mathbf{v}\cdot\nabla)Q_h, P_h)_{\Omega_h^n} - \frac{1}{2}((\mathbf{v}\cdot\nabla)P_h, Q_h)_{\Omega_h^n} + \frac{1}{2}((\boldsymbol{\nu}_h\cdot\mathbf{v})Q_h, P_h)_{\Gamma_h^n}, \\ A_h^n(Q_h, P_h) &= a_h^n(Q_h, P_h) + \gamma_{\mathrm{s}} s_h^n(Q_h, P_h), \\ l^n_{\mathrm{rhs},h}(P_h) &= \left(U^n_{\Omega,h}, P_h\right)_{\Omega_h^n} + w_0\left(Q^n_{\Gamma,h}, P_h\right)_{\Gamma_h^n} + w_1\left(-\frac{s_0}{3}\boldsymbol{\nu}_h\otimes\boldsymbol{\nu}_h, P_h\right)_{\Gamma_h^n} + \frac{2p_0}{3}(S, P_h)_{\Omega_h^n}. \end{aligned} \tag{82}$$

Furthermore, $U^n_{\Omega,h}$ and $Q^n_{\Gamma,h}$, are the interpolants of U^n_Ω and Q^n_Γ respectively that have been suitably extended such that the following estimates hold (see Assumption 1):

$$\|U^n_{\Omega,h} - U^n_\Omega\|_{H^1(\mathcal{O}(\Omega^n))} \approx h^q, \quad \|Q^n_{\Gamma,h} - Q^n_\Gamma\|_{H^1(\Gamma_h^n)} \approx h^q, \tag{83}$$

on some extended region $\mathcal{O}(\Omega^n)$ that contains Ω_h^n. Also, the velocity $\mathbf{v}$ is a suitable extension on $\mathcal{O}(\Omega^n)$ and for simplicity we assume that $\mathbf{v}$ is defined on the entire domain $\widehat{\mathfrak{D}}$.

We now state the weak formulation of the fully discrete, unfitted finite element scheme: Find $Q_h^n \in \mathbf{Q}_h(\Omega^n_{h,\delta})$ such that for all $P \in \mathbf{Q}_h(\Omega^n_{h,\delta})$ we have

$$\begin{aligned} &\int_{\Omega_h^n} \frac{1}{\triangle t} Q_h^n : P_h d\boldsymbol{x} + A_h^n(Q_h^n, P_h) + \frac{1}{\eta^2}(\psi'(Q_h^n), P_h)_{\Omega_h^n} + \frac{1}{\omega}(\phi'(Q_h^n), P_h)_{\Gamma_h^n} - (B(\nabla\mathbf{v}, Q_h^n), P_h)_{\Omega_h^n} \\ &\quad = l^n_{\mathrm{rhs},h}(P_h) + \int_{\Omega_h^n} \frac{1}{\triangle t} Q_h^{n-1} : P_h d\boldsymbol{x}, \end{aligned} \tag{84}$$

for each $n = 1, 2, ...N$. The following "coercivity" result is immediate.

Lemma 4. *For all* $Q_h \in \mathbb{S}_h(\Omega_h^n)$*, we have*

$$\begin{aligned} a_h^n(Q_h, Q_h) - (B(\nabla\mathbf{v}, Q_h), Q_h)_{\Omega_h^n} + \frac{1}{\eta^2}(\psi'(Q_h), Q_h)_{\Omega_h^n} + \frac{1}{\omega}(\phi'(Q_h), Q_h)_{\Gamma_h^n} \\ \geq \frac{\alpha_1}{4}\|\nabla Q_h\|^2_{L^2(\Omega_h^n)} + \frac{a_4}{4\eta^2}\|Q_h\|^4_{L^4(\Omega_h^n)} - \zeta_h'\|Q_h\|^2_{L^2(\Omega_h^n)}, \end{aligned} \tag{85}$$

where $\zeta_h' = \left[\frac{C^2_{\Omega_h^n}\zeta_1^2}{\alpha_1} + \zeta_2 - \frac{3\alpha_1}{4} - \frac{1}{2\eta^2}\right]$ *and* ζ_1*,* ζ_2 *are taken from Lemma 1.*

Proof. This is the same proof as in Lemma 1. □

The following unique solvability result is a discrete version of Theorem 2 and Corollary 1.

Theorem 3. *Assume* $\triangle t$ *satisfies* $0 < \triangle t < \max(\xi_0, 0)^{-1}$ *where* ξ_0 *is given by* (50)*. Then, for any* $n = 1, ..., N$*, there exists a* unique *solution of* (84)*.*

Proof. We introduce a discrete norm:

$$|||Q_h|||_n^2 := \|Q_h\|_{L^2(\Omega_h^n)}^2 + \frac{\alpha_1}{2}\|\nabla Q_h\|_{L^2(\Omega_h^n)}^2 + \gamma_s s_h^n(Q_h, Q_h), \tag{86}$$

and note that the bilinear form

$$\int_{\Omega_h^n} \frac{1}{\triangle t} Q_h : P_h d\boldsymbol{x} + A_h^n(Q_h, P_h)$$

is both continuous and coercive with respect to (86) under the assumed time step restriction. The rest of the proof is similar to the proofs of Theorem 2 and Corollary 1. ☐

We also have the discrete version of Lemma 2.

Theorem 4. *Let Q_h^n solve (84) for $n = 1, 2, ...N$. Then, we have the following stability estimate:*

$$\begin{aligned}(1 + C_2\triangle t)\|Q_h^k\|_{L^2(\Omega_h^k)}^2 + \triangle t \sum_{n=1}^{k}\left[\frac{\alpha_1}{8}\|Q_h^n\|_{H^1(\Omega_h^n)}^2 + \gamma_s \sum_{n=1}^{k} s_h(\mathcal{F}_{\Sigma_\delta^\pm}^n; Q_h^n, Q_h^n)\right] \\ \leq C_1\|Q_h^0\|_{L^2(\Omega_h^0)}^2 + D_h, \text{ for all } k = 1, ..., N,\end{aligned} \tag{87}$$

where $D_h = \triangle t \sum_{n=1}^{N}\left[\|U_\Omega^n\|_{L^2(\Omega_h^n)}^2 + w_0^2\|Q_\Gamma^n\|_{L^2(\Gamma_h^n)}^2 + \frac{w_1^2 s_0^2}{9}|\Gamma_h^n|^2 + \frac{4p_0^2}{9}\|S\|_{L^2(\Omega_h^n)}^2 + \frac{\eta^2}{2a_4}\kappa_0^2|\Omega_h^n|\right]$ *with* $\zeta_h'' = \left[2\zeta_h' + \frac{4C_{\Omega_h^n}^2}{\alpha_1} + \frac{\alpha_1}{4} + 2\right]$ *and* $\kappa_0 = \max(0, \zeta_h'' + C_2 + \alpha_1/4)$*, where ζ_h' is taken from Lemma 4.*

Proof. The proof is an obvious modification of the proof of Lemma 2 to account for the facet stabilization; see the definition of $A_h^n(\cdot, \cdot)$ in (82). ☐

5 Error Analysis for the Fully Discrete Method

5.1 Geometry Approximation

Recall from Section 2.3 that $\Gamma(t) = \partial\Omega(t) = \partial\widehat{\mathfrak{D}} \cup \widetilde{\Gamma}(t)$, where $\widetilde{\Gamma}(t) \in C^{m+1}$, for some $m \geq 1$, is the smooth inner boundary. *For technical convenience* in this section, we assume that all of $\Gamma(t)$ is C^{m+1}. This implies that we have solution regularity $Q(\cdot, t) \in H^{m+1}(\Omega(t); \mathbf{S}_0)$ for all $t \in [0, T]$, and by the extension operator in Section A.1, we consider Q to be extended onto $\widehat{\mathfrak{D}}$ with $Q(\cdot, t) \in H^{m+1}(\widehat{\mathfrak{D}}; \mathbf{S}_0)$ for all $t \in [0, T]$. Of course, if the outer boundary $\partial\widehat{\mathfrak{D}}$ is only convex, then we are limited to $H^2(\widehat{\mathfrak{D}}; \mathbf{S}_0)$ regularity.

We codify the geometric approximation in the following assumption.

Assumption 1. *We assume that $\Omega_h^n \equiv \Omega_h(t_n)$ is the sub-zero level set of a discrete level set function $\phi_h(t_n, \cdot)$ having polynomial degree q such that $m \geq q \geq 1$, and that Ω_h^n approximates $\Omega^n \equiv \Omega(t_n)$ to order q as described in* (88)*,* (89)*, and* (90)*. We also define our finite element space $\mathbf{Q}_h$ to contain piecewise polynomials of up to order m.*

For describing the geometric approximation results, we temporarily suppress the time index notation. Following the same approach as in [22] and [34], we have an approximation of the discrete domain Ω_h, with the discrete level set function ϕ_h, satisfying

$$\operatorname{dist}(\Omega, \Omega_h) \lesssim h^{q+1}, \tag{88}$$

where $q \geq 1$ is the order of the geometry approximation (i.e. q is the polynomial degree of ϕ_h). In addition, we assume that there exists a mapping $\mathbf{\Phi} : \mathcal{O}_{\delta_h}(\Omega_h) \to \mathcal{O}_{\delta_h}(\Omega)$ (uniform in t) with the following properties:

$$\begin{gathered}\mathbf{\Phi}(\Omega_h) = \Omega, \quad \mathbf{\Phi}(\mathcal{O}_{\delta_h}(\Omega_h)) = \mathcal{O}_{\delta_h}(\Omega), \\ \|\mathbf{\Phi} - \mathbf{id}\|_{L^\infty(\mathcal{O}_{\delta_h}(\Omega_h))} \lesssim h^{q+1}, \quad \|\nabla\mathbf{\Phi} - I\|_{L^\infty(\mathcal{O}_{\delta_h}(\Omega_h))} \lesssim h^q, \quad \|\det(\nabla\mathbf{\Phi}) - 1\|_{L^\infty(\mathcal{O}_{\delta_h}(\Omega_h))} \lesssim h^q,\end{gathered} \tag{89}$$

where $\mathbf{\Phi}$ is a continuous well-defined map that is invertible for sufficiently small h (and uniformly in t), and $\boldsymbol{\nu} = \nabla\phi/|\nabla\phi|$ on Γ, $\boldsymbol{\nu}_h = \nabla\phi_h/|\nabla\phi_h|$ on Γ_h. Moreover, for surface elements, we note the following estimates from [22]

$$dS(\mathbf{\Phi}(\boldsymbol{a})) = \mu_h dS(\boldsymbol{a}), \quad \|\mu_h - 1\|_{L^\infty(\Gamma_h)} \lesssim h^q, \quad \|\boldsymbol{\nu} - \boldsymbol{\nu}_h\|_{L^\infty(\Gamma_h)} \lesssim h^q. \tag{90}$$

where dS_h (dS) represents the Lebesgue measure for Γ_h (Γ). We abuse notation and use dS for either Γ or Γ_h depending on the context. The function μ_h is the Jacobian resulting from the change of variables for the surface integral.

For any $Q_h \in \mathbf{Q}_h$, we define $Q_h^\ell := Q_h \circ \mathbf{\Phi}^{-1}$ and note the following estimates:

$$\begin{aligned} \|Q_h^\ell\|^2_{L^2(\mathcal{O}_{\delta_h}(\Omega^n))} &\simeq \|Q_h\|^2_{L^2(\mathcal{O}_{\delta_h}(\Omega_h^n))}, \qquad \|Q_h^\ell\|^2_{L^2(\Omega^n)} \simeq \|Q_h\|^2_{L^2(\Omega_h^n)}, \\ \|\nabla Q_h^\ell\|^2_{L^2(\mathcal{O}_{\delta_h}(\Omega^n))} &\simeq \|\nabla Q_h\|^2_{L^2(\mathcal{O}_{\delta_h}(\Omega_h^n))}, \qquad \|\nabla Q_h^\ell\|^2_{L^2(\Omega^n)} \simeq \|\nabla Q_h\|^2_{L^2(\Omega_h^n)}. \end{aligned} \tag{91}$$

We also collect some basic estimates in Appendix A.2 that will be used repeatedly.

5.2 Consistency Estimate

Taking (29), and setting $t = t_n$, we have

$$\int_{\Omega^n} \partial_t Q^n : P d\boldsymbol{x} + a^n(Q^n, P) + \frac{1}{\eta^2}(\psi'(Q^n), P)_{\Omega^n} + \frac{1}{\omega}(\phi'(Q^n), P)_{\Gamma^n} - (B(\nabla\mathbf{v}, Q^n), P)_{\Omega^n} = l^n_{\text{rhs}}(P), \tag{92}$$

and we choose $P = P_h^\ell := P_h \circ \mathbf{\Phi}^{-1}$ for arbitrary $P_h \in \mathbf{Q}_h$. Now, subtracting (84) from (92), we get the following:

$$\int_{\Omega_h^n} \frac{\mathbb{E}^n - \mathbb{E}^{n-1}}{\triangle t} : P_h d\boldsymbol{x} + a_h^n(\mathbb{E}^n, P_h) + \gamma_{\text{s}} s_h(\mathcal{F}^n_{\Sigma_\delta^\pm}; \mathbb{E}^n, P_h) = \mathcal{E}_0(P_h) + \mathcal{E}_B(P_h) + \mathcal{E}_\psi(P_h) + \mathcal{E}_\phi(P_h), \tag{93}$$

where we have the following definitions

$$\begin{aligned} \mathbb{E}^n &:= Q^n - Q_h^n \quad \forall n, \\ \mathcal{E}_0(P_h) &:= \mathcal{E}_1(P_h) + \mathcal{E}_2(P_h) + \mathcal{E}_3(P_h) + \mathcal{E}_4(P_h), \\ \mathcal{E}_1(P_h) &:= \int_{\Omega_h^n} \frac{Q^n - Q^{n-1}}{\triangle t} : P_h d\boldsymbol{x} - \int_{\Omega^n} \partial_t Q^n : P_h^\ell d\boldsymbol{x}, \\ \mathcal{E}_2(P_h) &:= a_h^n(Q^n, P_h) - a^n\left(Q^n, P_h^\ell\right), \\ \mathcal{E}_3(P_h) &:= \gamma_{\text{s}} s_h(\mathcal{F}^n_{\Sigma_\delta^\pm}; Q^n, P_h), \\ \mathcal{E}_4(P_h) &:= l^n_{\text{rhs}}(P_h^\ell) - l^n_{\text{rhs},h}(P_h), \\ \mathcal{E}_B(P_h) &:= \left(B(\nabla\mathbf{v}, Q^n), P_h^\ell\right)_{\Omega^n} - (B(\nabla\mathbf{v}, Q_h^n), P_h)_{\Omega_h^n} \\ \mathcal{E}_\psi(P_h) &:= \frac{1}{\eta^2}\int_{\Omega_h^n} \psi'(Q_h^n) : P_h d\boldsymbol{x} - \frac{1}{\eta^2}\int_{\Omega^n} \psi'(Q^n) : P_h^\ell d\boldsymbol{x}, \\ \mathcal{E}_\phi(P_h) &:= \frac{1}{\omega}\int_{\Gamma_h^n} \phi'(Q_h^n) : P_h dS - \frac{1}{\omega}\int_{\Gamma^n} \phi'(Q^n) : P_h^\ell dS. \end{aligned} \tag{94}$$

Recall the decomposition $Q^n = q_i^n E^i$ and we define the Lagrange interpolant of Q^n denoted by $Q_I^n \in \mathbf{Q}_h$ by taking the Lagrange interpolant componentwise of $\mathbf{q}^n = (q_1^n, q_2^n, q_3^n, q_4^n, q_5^n)^T$. Now we further split (93) using the Lagrange interpolant Q_I^n given that Q^n is sufficiently smooth. Next, define

$$\mathbb{E}^n \equiv \underbrace{Q^n - Q_I^n}_{e^n} + \underbrace{Q_I^n - Q_h^n}_{e_h^n \in \mathbf{Q}_h} \quad \forall n. \tag{95}$$

Then, we get the following

$$\int_{\Omega_h^n} \frac{e_h^n - e_h^{n-1}}{\triangle t} : P_h d\boldsymbol{x} + a_h^n(e_h^n, P_h) + \gamma_{\text{s}} s_h(\mathcal{F}^n_{\Sigma_\delta^\pm}; e_h^n, P_h) = \mathcal{E}_I(P_h) + \mathcal{E}_0(P_h) + \mathcal{E}_B(P_h) + \mathcal{E}_\psi(P_h) + \mathcal{E}_\phi(P_h), \tag{96}$$

where

$$\mathcal{E}_I(P_h) := -\int_{\Omega_h^n} \frac{e^n - e^{n-1}}{\triangle t} : P_h d\boldsymbol{x} - a_h^n\left(e^n, P_h\right) - \gamma_{\mathrm{s}} s_h(\mathcal{F}^n_{\Sigma^{\pm}_\delta}; e^n, P_h). \tag{97}$$

Lemma 5. *Assume the following regularity of the exact solution:*

$$Q \in W^{2,\infty}(\mathcal{C}) \cap L^\infty([0,T]; H^{m+1}(\Omega(t))), \quad \partial_t Q \in L^\infty([0,T]; H^m(\Omega(t))),$$

where $\mathcal{C} := \bigcup_{t\in(0,T)} \Omega(t) \times \{t\}$ *is the space-time cylinder. For any* $\eta > 0$*, we have an estimate for* $\mathcal{E}_I(P_h)$*:*

$$|\mathcal{E}_I(P_h)| \lesssim \frac{\eta}{2} h^{2m} K \sup_{t\in[0,T]} \left(\|Q\|^2_{H^{m+1}(\Omega(t))} + \|Q_t\|^2_{H^m(\Omega(t))}\right) + \frac{1}{2\eta}\left[\|P_h\|^2_{H^1(\Omega_h^n)} + s_h^n\left(P_h, P_h\right)\right].$$

Proof. The proof follows from Proposition 2, and (17), and applying Lemma 5.12 in [34] to each component of Q along with a weighted Young's inequality. □

Lemma 6. *Assume* $Q \in W^{2,\infty}(\mathcal{C}) \cap L^\infty([0,T]; H^{m+1}(\Omega(t)))$ *and Assumption 1. Then, we have the following estimate for* $\mathcal{E}_0(P_h)$ *for each* $n = 1, ..., N$*:*

$$\begin{aligned}|\mathcal{E}_0(P_h)| \lesssim [\triangle t + h^q + h^m] \Big[&\|Q^n\|_{W^{2,\infty}(\mathcal{C})} + \sup_{t\in[0,T]} \|Q\|_{H^{m+1}(\Omega(t))} \\ &+ \|U^n_\Omega\|_{H^1(\Omega_h^n)} + \|\mathbf{v}\|_{W^{2,\infty}(\mathcal{C})} + \|Q^n_\Gamma\|_{H^2(\Omega_h^n)} + C\Big]\left[\|P_h\|_{H^1(\Omega_h^n)} + s_h^n\left(P_h, P_h\right)^{1/2}\right].\end{aligned}$$

Proof. For $\mathcal{E}_1(P_h)$ we use Taylor's Theorem with the integral form of the remainder:

$$Q(\boldsymbol{x}, t_{n-1}) = Q(\boldsymbol{x}, t_n) + Q_t(\boldsymbol{x}, t_n)(t_{n-1} - t_n) + \int_{t_n}^{t_{n-1}} Q_{tt}(t, \boldsymbol{x})(t_{n-1} - t)dt.$$

Then, upon noting that Q^n is extended for all n, we have

$$\begin{aligned}\mathcal{E}_1(P_h) &= \int_{\Omega_h^n} \frac{Q^n - Q^{n-1}}{\triangle t} : P_h d\boldsymbol{x} - \int_{\Omega^n} Q_t^n : P_h^\ell d\boldsymbol{x} \\ &= \int_{\Omega_h^n} Q_t(\boldsymbol{x}, t_n) : P_h + \int_{t_{n-1}}^{t_n} \frac{(t_{n-1} - t)}{\triangle t} Q_{tt}(\boldsymbol{x}, t) : P_h dt d\boldsymbol{x} - \int_{\Omega^n} Q_t^n : P_h^\ell d\boldsymbol{x} \\ &= \int_{\Omega_h^n}\int_{t_{n-1}}^{t_n} \frac{(t_{n-1} - t)}{\triangle t} Q_{tt}(\boldsymbol{x}, t) dt : P_h d\boldsymbol{x} + \int_{\Omega_h^n} Q_t(\boldsymbol{x}, t_n) : P_h d\boldsymbol{x} - \int_{\Omega^n} Q_t^n : P_h^\ell d\boldsymbol{x} \\ &= \int_{\Omega_h^n}\int_{t_{n-1}}^{t_n} \frac{(t_{n-1} - t)}{\triangle t} Q_{tt}(\boldsymbol{x}, t) dt : P_h d\boldsymbol{x} + \int_{\Omega_h^n} Q_t(\boldsymbol{x}, t_n) : P_h d\boldsymbol{x} - \int_{\Omega_h^n} (Q_t^n \circ \boldsymbol{\Phi}) : P_h \det(\nabla\boldsymbol{\Phi}) d\boldsymbol{x},\end{aligned} \tag{98}$$

where in the last line we performed a change of variables. And now we split the above into two parts:

$$\begin{aligned}\left|\int_{\Omega_h^n}\int_{t_{n-1}}^{t_n} \frac{(t_{n-1} - t)}{\triangle t} Q_{tt}(\boldsymbol{x}, t) dt : P_h d\boldsymbol{x}\right| &\le \frac{1}{\triangle t}\|Q_{tt}\|_{L^\infty(\mathcal{O}_{\delta_h}(\mathcal{C}))}\|P_h\|_{L^1(\Omega_h^n)} \int_{t_{n-1}}^{t_n} |t_{n-1} - t| dt \\ &= \frac{1}{\triangle t}\|Q_{tt}\|_{L^\infty(\mathcal{O}_{\delta_h}(\mathcal{C}))}\|P_h\|_{L^1(\Omega_h^n)} \frac{1}{2}\triangle t^2 \\ &\lesssim \triangle t \|Q\|_{W^{2,\infty}(\mathcal{C})}\|P_h\|_{L^2(\Omega_h^n)},\end{aligned} \tag{99}$$

where we have used Hölder's inequality and some standard techniques. Next,

$$\begin{aligned}
&\left|\int_{\Omega_h^n} Q_t(\boldsymbol{x},t_n) : P_h d\boldsymbol{x} - \int_{\Omega_h^n} (Q_t^n \circ \boldsymbol{\Phi}) : P_h \det(\nabla \boldsymbol{\Phi}) d\boldsymbol{x}\right| \\
\leq &\left|\int_{\Omega_h^n} Q_t^n : P_h - (Q_t^n \circ \boldsymbol{\Phi}) : P_h d\boldsymbol{x}\right| + h^q \int_{\Omega_h^n} |(Q_t^n \circ \boldsymbol{\Phi}) : P_h| d\boldsymbol{x} \\
\lesssim & h^{q+1} \left\|\nabla Q_t^n\right\|_{L^\infty(\mathcal{O}_{\delta_h}(\Omega_h^n))} \|P_h\|_{L^1(\Omega_h^n)} + h^q \|Q_t^n\|_{L^\infty(\mathcal{O}_{\delta_h}(\Omega_h^n))} \|P_h\|_{L^1(\Omega_h^n)} \\
\lesssim & h^q \|Q\|_{W^{2,\infty}(\mathcal{C})} \|P_h\|_{L^2(\Omega_h^n)},
\end{aligned} \tag{100}$$

where we have used the fundamental theorem of calculus for line integrals, Lemma 13, the geometry approximation between the discrete and exact domains, and some other standard estimates.

Next, we consider $\mathcal{E}_2(P_h) = a_h^n(Q^n, P_h) - a^n\left(Q^n, P_h^\ell\right)$ and split it with the triangle inequality:

$$\begin{aligned}
|\mathcal{E}_2(P_h)| &\leq I_1 + I_2 + I_3 + I_4 + I_5, \\
I_1 &:= \left|(\mathcal{A}\nabla Q^n, \nabla P_h)_{\Omega_h^n} - \left(\mathcal{A}\nabla Q^n, \nabla P_h^\ell\right)_{\Omega^n}\right|, \\
I_2 &:= \left|a_{\mathrm{s}}\left(\Omega_h^n; Q^n, P_h\right) - a_{\mathrm{s}}\left(\Omega^n; Q^n, P_h^\ell\right)\right|, \\
I_3 &:= \frac{1}{2}\left|\int_{\Omega_h^n} (\mathbf{v}\cdot\nabla Q^n) : P_h d\boldsymbol{x} - \int_{\Omega^n} (\mathbf{v}\cdot\nabla Q^n) : P_h^\ell d\boldsymbol{x}\right|, \\
I_4 &:= \frac{1}{2}\left|\int_{\Omega_h^n} (\mathbf{v}\cdot\nabla P_h) : Q^n d\boldsymbol{x} - \int_{\Omega^n} (\mathbf{v}\cdot\nabla P_h^\ell) : Q^n d\boldsymbol{x}\right|, \\
I_5 &:= \frac{1}{2}\left|\int_{\Gamma_h^n} (\boldsymbol{\nu}_h\cdot\mathbf{v}) Q^n : P_h dS - \int_{\Gamma^n} (\boldsymbol{\nu}\cdot\mathbf{v}) Q^n : P_h^\ell dS\right|.
\end{aligned}$$

Estimating the first term, we have

$$\begin{aligned}
I_1 &= \left|(\mathcal{A}\nabla Q^n, \nabla P_h)_{\Omega_h^n} - \left(\mathcal{A}\nabla Q^n, \nabla P_h^\ell\right)_{\Omega^n}\right| \\
&= \left|\int_{\Omega_h^n} (\mathcal{A}\nabla Q^n) \vdots \nabla P_h - (\mathcal{A}(\nabla Q^n \circ \boldsymbol{\Phi})) \vdots (\nabla P_h^\ell) \circ \boldsymbol{\Phi} \det(\nabla\boldsymbol{\Phi}) d\boldsymbol{x}\right| \\
&\lesssim \left|\int_{\Omega_h^n} (\mathcal{A}\nabla Q^n) \vdots \nabla P_h - (\mathcal{A}(\nabla Q^n \circ \boldsymbol{\Phi})) \vdots (\nabla P_h^\ell) \circ \boldsymbol{\Phi} d\boldsymbol{x}\right| + h^q \|(\mathcal{A}(\nabla Q^n \circ \boldsymbol{\Phi})) \vdots (\nabla P_h^\ell) \circ \boldsymbol{\Phi}\|_{L^1(\Omega_h^n)} \\
&\lesssim \left|\int_{\Omega_h^n} (\mathcal{A}\nabla Q^n) \vdots \nabla P_h - (\mathcal{A}(\nabla Q^n \circ \boldsymbol{\Phi})) \vdots (\nabla\boldsymbol{\Phi})^{-1} \nabla P_h d\boldsymbol{x}\right| + h^q \|\mathcal{A}\|_\infty \|\nabla Q^n\|_{L^\infty(\Omega^n)} \|(\nabla\boldsymbol{\Phi})^{-1}\nabla P_h\|_{L^1(\Omega_h^n)} \\
&\lesssim \left|\int_{\Omega_h^n} (\mathcal{A}\nabla Q^n) \vdots \nabla P_h - (\mathcal{A}(\nabla Q^n \circ \boldsymbol{\Phi})) \vdots \nabla P_h d\boldsymbol{x}\right| + h^q \|\mathcal{A}\|_\infty \|Q\|_{W^{2,\infty}(\mathcal{C})} \|P_h\|_{H^1(\Omega_h^n)} \\
&\lesssim h^{q+1} \|\nabla(\mathcal{A}\nabla Q^n)\|_{L^\infty(\mathcal{O}_{\delta_h}(\Omega_h^n))} \|\nabla P_h\|_{L^1(\Omega_h^n)} + h^q \|\mathcal{A}\|_\infty \|Q\|_{W^{2,\infty}(\mathcal{C})} \|P_h\|_{H^1(\Omega_h^n)} \\
&\lesssim h^{q+1} \|\mathcal{A}\|_\infty \|\nabla^2 Q^n\|_{L^\infty(\Omega_h^n)} \|P_h\|_{H^1(\Omega_h^n)} + h^q \|\mathcal{A}\|_\infty \|Q\|_{W^{2,\infty}(\mathcal{C})} \|P_h\|_{H^1(\Omega_h^n)} \\
&\lesssim h^q \|Q\|_{W^{2,\infty}(\mathcal{C})} \|P_h\|_{H^1(\Omega_h^n)},
\end{aligned} \tag{101}$$

where we used a basic change of variables and Lemmas 10, 11, and 12. The estimates for I_2, I_3, and I_4 follow from a very similar method. Lastly, for I_5 we have

$$
\begin{aligned}
I_5 &= \frac{1}{2}\left|\int_{\Gamma_h^n}(\boldsymbol{\nu}_h\cdot\mathbf{v})Q^n : P_h dS - \int_{\Gamma^n}(\boldsymbol{\nu}\cdot\mathbf{v})Q^n : P_h^\ell dS\right| \\
&= \frac{1}{2}\left|\int_{\Gamma_h^n}(\boldsymbol{\nu}_h\cdot\mathbf{v})Q^n : P_h - (\boldsymbol{\nu}_h\cdot(\mathbf{v}\circ\mathbf{\Phi}))(Q^n\circ\mathbf{\Phi}) : P_h\mu_h dS\right| \\
&\lesssim \left|\int_{\Gamma_h^n}(\boldsymbol{\nu}_h\cdot\mathbf{v})Q^n : P_h - (\boldsymbol{\nu}_h\cdot(\mathbf{v}\circ\mathbf{\Phi}))(Q^n\circ\mathbf{\Phi}) : P_h dS\right| + h^q\|(\mathbf{v}\circ\mathbf{\Phi})(Q^n\circ\mathbf{\Phi})P_h\|_{L^1(\Gamma_h^n)} \\
&\lesssim h^{q+1}\|\nabla[(\boldsymbol{\nu}\cdot\mathbf{v})Q^n]\|_{L^\infty(\mathcal{O}_{\delta_h}(\Omega_h^n))}\|P_h\|_{L^1(\Gamma_h^n)} + h^q\|\mathbf{v}\|_{L^\infty(\Gamma^n)}\|Q^n\|_{L^\infty(\Gamma^n)}\|P_h\|_{L^1(\Gamma_h^n)} \\
&\lesssim h^{q+1}\|\mathbf{v}\|_{W^{1,\infty}(\Omega^n)}\|Q\|_{W^{2,\infty}(\mathcal{C})}\|P_h\|_{H^1(\Omega_h^n)} + h^q\|\mathbf{v}\|_{L^\infty(\Gamma^n)}\|Q\|_{W^{2,\infty}(\mathcal{C})}\|P_h\|_{H^1(\Omega_h^n)} \\
&\lesssim h^q\|Q\|_{W^{2,\infty}(\mathcal{C})}\|P_h\|_{H^1(\Omega_h^n)}.
\end{aligned}
$$

Then, putting everything together we get:

$$
|\mathcal{E}_2(P_h)| \lesssim h^q\|Q\|_{W^{2,\infty}(\mathcal{C})}\|P_h\|_{H^1(\Omega_h^n)}.
$$

Now, we handle $\mathcal{E}_3(P_h)$ using a Cauchy-Schwarz inequality and [34, Lem. 5.8]:

$$
\begin{aligned}
|\mathcal{E}_3(P_h)| &= |\gamma_{\mathrm{s}} s_h(\mathcal{F}^n_{\Sigma_\delta^\pm}; Q^n, P_h)| \le \gamma_{\mathrm{s}} s_h(\mathcal{F}^n_{\Sigma_\delta^\pm}; Q^n, Q^n)^{1/2} s_h(\mathcal{F}^n_{\Sigma_\delta^\pm}; P_h, P_h)^{1/2} \\
&\lesssim h^m\|Q\|_{H^{m+1}(\mathfrak{O}^n_{\delta_h})} s_h(\mathcal{F}^n_{\Sigma_\delta^\pm}; P_h, P_h)^{1/2} \lesssim h^m\|Q\|_{H^{m+1}(\Omega^n)} s_h(\mathcal{F}^n_{\Sigma_\delta^\pm}; P_h, P_h)^{1/2}.
\end{aligned} \tag{102}
$$

Next, we estimate $\mathcal{E}_4(P_h)$:

$$
\begin{aligned}
|\mathcal{E}_4(P_h)| \le &\left|\left(U_\Omega^n\circ\mathbf{\Phi} - U_{\Omega,h}^n, P_h\right)_{\Omega_h^n}\right| + \frac{2p_0}{3}\left|(S\circ\mathbf{\Phi} - S, P_h)_{\Omega_h^n}\right| \\
&+ \left|w_0\left(Q_\Gamma^n\circ\mathbf{\Phi} - Q_{\Gamma,h}^n, P_h\right)_{\Gamma_h^n}\right| + w_1\frac{s_0}{3}\left|((\boldsymbol{\nu}\otimes\boldsymbol{\nu})\circ\mathbf{\Phi} - \boldsymbol{\nu}_h\otimes\boldsymbol{\nu}_h, P_h)_{\Gamma_h^n}\right|,
\end{aligned} \tag{103}
$$

where we applied a change of variables. Proceeding analogously to our other estimates, we obtain

$$
\begin{aligned}
|\mathcal{E}_4(P_h)| &\lesssim h^q\left(\|U_\Omega^n\|_{H^1(\Omega_h^n)} + \|\mathbf{v}\|_{W^{2,\infty}(\Omega^n)}\right)\|P_h\|_{L^2(\Omega_h^n)} + h^q\left(\|Q_\Gamma^n\|_{H^2(\Omega_h^n)} + C\right)\|P_h\|_{H^1(\Omega_h^n)} \\
&\lesssim h^q\left[\|U_\Omega^n\|_{H^1(\Omega_h^n)} + \|\mathbf{v}\|_{W^{2,\infty}(\Omega^n)} + \|Q_\Gamma^n\|_{H^2(\Omega_h^n)} + C\right]\|P_h\|_{H^1(\Omega_h^n)},
\end{aligned}
$$

where C depends on the regularity of $\boldsymbol{\nu}$. □

Next, we bound the consistency error for the Beris–Edwards term.

Lemma 7. *Assume $Q^n \in H^{m+1}(\Omega^n)$ and Assumption 1. Then, we have the following estimate:*

$$
\begin{aligned}
|\mathcal{E}_B(P_h)| \lesssim &\|\nabla\mathbf{v}\|_{L^\infty(\widehat{\mathfrak{D}})}\|Q_I^n - Q_h^n\|_{L^2(\Omega_h^n)}\left(1 + \|Q^n\|_{L^4(\Omega_h^n)} + \|Q_h^n\|_{L^4(\Omega_h^n)}\right)\|P_h\|_{H^1(\Omega_h^n)} \\
&+ (h^{m+1} + h^{q+1})\|\nabla\mathbf{v}\|_{L^\infty(\widehat{\mathfrak{D}})}\|Q^n\|_{H^{m+1}(\Omega_h^n)}\left(1 + \|Q^n\|_{L^4(\Omega_h^n)}\right)\|P_h\|_{H^1(\Omega_h^n)} \\
&+ h^q\|\mathbf{v}\|_{W^{2,\infty}(\widehat{\mathfrak{D}})}\left[\|Q^n\|_{L^2(\Omega_h^n)} + \|Q^n\|^2_{L^4(\Omega_h^n)}\right]\|P_h\|_{L^2(\Omega_h^n)}.
\end{aligned} \tag{104}
$$

Proof. We first note the following identity:

$$
\mathcal{E}_B(P_h) = \underbrace{\left(B\left(\nabla\mathbf{v}, Q_I^n\right), P_h\right)_{\Omega_h^n} - \left(B\left(\nabla\mathbf{v}, Q_h^n\right), P_h\right)_{\Omega_h^n}}_{=:\mathcal{E}_B^1(P_h)} + \underbrace{\left(B\left(\nabla\mathbf{v}, Q^n\right), P_h^\ell\right)_{\Omega^n} - \left(B\left(\nabla\mathbf{v}, Q_I^n\right), P_h\right)_{\Omega_h^n}}_{=:\mathcal{E}_B^2(P_h)}.
$$

Estimating $\mathcal{E}_B^1(P_h)$ delivers

$$
\begin{aligned}
\left|\mathcal{E}_B^1(P_h)\right| &\leq \left|\int_{\Omega_h^n} \left[B\left(\nabla\mathbf{v}, Q_I^n\right) - B\left(\nabla\mathbf{v}, Q_h^n\right)\right] : P_h d\boldsymbol{x}\right| \\
&\leq \|\nabla\mathbf{v}\|_{L^\infty(\widehat{\mathfrak{D}})} \|Q_I^n - Q_h^n\|_{L^2(\Omega_h^n)} \|P_h\|_{L^2(\Omega_h^n)} + 2\int_{\Omega_h^n} \left[(S : Q_I^n)(Q_I^n - Q_h^n) + (S : (Q_I^n - Q_h^n))Q_h^n\right] : P_h d\boldsymbol{x} \\
&\lesssim \|\nabla\mathbf{v}\|_{L^\infty(\widehat{\mathfrak{D}})} \|Q_I^n - Q_h^n\|_{L^2(\Omega_h^n)} \left(1 + \|Q^n\|_{L^4(\Omega_h^n)} + \|Q_h^n\|_{L^4(\Omega_h^n)}\right) \|P_h\|_{H^1(\Omega_h^n)},
\end{aligned}
$$

where we used a Hölder inequality. Then, using a change of variables, we have

$$
\begin{aligned}
\left|\mathcal{E}_B^2(P_h)\right| \leq& \left|\int_{\Omega_h^n} \left[B\left(\nabla\mathbf{v}, Q^n\right) - B\left(\nabla\mathbf{v}, Q_I^n\right)\right] : P_h d\boldsymbol{x}\right| + \left|\int_{\Omega_h^n} \left[B\left(\nabla\mathbf{v}\circ\boldsymbol{\Phi}, Q^n\circ\boldsymbol{\Phi}\right) - B\left(\nabla\mathbf{v}, Q^n\right)\right] : P_h d\boldsymbol{x}\right| \\
&+ \left|\int_{\Omega_h^n} B\left(\nabla\mathbf{v}\circ\boldsymbol{\Phi}, Q^n\circ\boldsymbol{\Phi}\right) : P_h[\det(\nabla\boldsymbol{\Phi}) - 1] d\boldsymbol{x}\right| = I_1 + I_2 + I_3.
\end{aligned}
$$

Estimating I_1, similar to $\left|\mathcal{E}_B^1(P_h)\right|$, yields

$$
I_1 \lesssim \|\nabla\mathbf{v}\|_{L^\infty(\widehat{\mathfrak{D}})} \|Q^n - Q_I^n\|_{L^2(\Omega_h^n)} \left(1 + \|Q^n\|_{L^4(\Omega_h^n)}\right) \|P_h\|_{H^1(\Omega_h^n)}.
$$

Next, we estimate I_2:

$$
\begin{aligned}
I_2 \leq& \left|\int_{\Omega_h^n} \left[B\left(\nabla\mathbf{v}\circ\boldsymbol{\Phi}, Q^n\circ\boldsymbol{\Phi}\right) - B\left(\nabla\mathbf{v}, Q^n\circ\boldsymbol{\Phi}\right)\right] : P_h d\boldsymbol{x}\right| + \left|\int_{\Omega_h^n} \left[B\left(\nabla\mathbf{v}, Q^n\circ\boldsymbol{\Phi}\right) - B\left(\nabla\mathbf{v}, Q^n\right)\right] : P_h d\boldsymbol{x}\right| \\
\lesssim& h^{q+1} \|\mathbf{v}\|_{W^{2,\infty}(\widehat{\mathfrak{D}})} \left[\|Q^n\|_{L^2(\mathcal{O}_{\delta_h}(\Omega_h^n))} + \|Q^n\|^2_{L^4(\mathcal{O}_{\delta_h}(\Omega_h^n))}\right] \|P_h\|_{L^2(\Omega_h^n)} \\
&+ \|\nabla\mathbf{v}\|_{L^\infty(\widehat{\mathfrak{D}})} \|Q^n\circ\boldsymbol{\Phi} - Q^n\|_{L^2(\Omega_h^n)} \left(\|P_h\|_{L^2(\Omega_h^n)} + \|Q^n\|_{L^4(\mathcal{O}_{\delta_h}(\Omega_h^n))} \|P_h\|_{L^4(\Omega_h^n)}\right) \\
\lesssim& h^{q+1} \|\mathbf{v}\|_{W^{2,\infty}(\widehat{\mathfrak{D}})} \left[\|Q^n\|_{L^2(\mathcal{O}_{\delta_h}(\Omega_h^n))} + \|Q^n\|^2_{L^4(\mathcal{O}_{\delta_h}(\Omega_h^n))}\right] \|P_h\|_{L^2(\Omega_h^n)} \\
&+ \|\nabla\mathbf{v}\|_{L^\infty(\widehat{\mathfrak{D}})} h^{q+1} \|\nabla Q^n\|_{L^2(\mathcal{O}_{\delta_h}(\Omega_h^n))} \left(\|P_h\|_{L^2(\Omega_h^n)} + \|Q^n\|_{L^4(\mathcal{O}_{\delta_h}(\Omega_h^n))} \|P_h\|_{L^4(\Omega_h^n)}\right),
\end{aligned}
$$

where we used properties of the extension. As for I_3, using the geometric approximation, we get

$$
\begin{aligned}
I_3 &\lesssim h^q \left|\int_{\Omega_h^n} B\left(\nabla\mathbf{v}\circ\boldsymbol{\Phi}, Q^n\circ\boldsymbol{\Phi}\right) : P_h d\boldsymbol{x}\right| \\
&\lesssim h^q \|\mathbf{v}\|_{W^{1,\infty}(\widehat{\mathfrak{D}})} \left[\|Q^n\|_{L^2(\mathcal{O}_{\delta_h}(\Omega_h^n))} + \|Q^n\|^2_{L^4(\mathcal{O}_{\delta_h}(\Omega_h^n))}\right] \|P_h\|_{L^2(\Omega_h^n)}.
\end{aligned}
$$

Then, taking advantage of the regularity of Q^n and interpolation theory, we note that

$$
\|Q^n - Q_I^n\|_{L^2(\Omega_h^n)} \lesssim h^{m+1} \|Q^n\|_{H^{m+1}(\Omega_h^n)}.
$$

Then, using the properties of the extension and combining the results, we obtain (104). □

The next two lemmas are needed to deal with the nonlinearities and the convex splittings of the double well potentials.

Lemma 8. *Assume $Q^n \in H^{m+1}(\Omega)$ for $m \geq 1$ and Assumption 1. Then, we have the following estimates:*

$$
\begin{aligned}
&\eta^2 \mathcal{E}_\psi(P_h) = (\psi'(Q_h^n) - \psi'(Q_I^n), P_h)_{\Omega_h^n} + \eta^2 \widetilde{\mathcal{E}_\psi}(P_h), \\
&\left|\eta^2 \widetilde{\mathcal{E}_\psi}(P_h)\right| \lesssim h^{m+1} \|Q^n\|_{H^{m+1}(\Omega_h^n)} \|P_h\|_{H^1(\Omega_h^n)} + h^{q+1} \|\nabla Q^n\|_{L^2(\Omega_h^n)} \|P_h\|_{H^1(\Omega_h^n)} + \widehat{C} h^q \|P_h\|_{L^2(\Omega_h^n)},
\end{aligned} \tag{105}
$$

where the (implicit) constants in the inequality, and $\widehat{C} > 0$, depend on $\|Q^n\|_{H^2(\Omega_h^n)}$.

Proof. We first note the following identity:

$$\eta^2 \mathcal{E}_\psi(P_h) = (\psi'(Q_h^n) - \psi'(Q_I^n), P_h)_{\Omega_h^n} + \underbrace{(\psi'(Q_I^n), P_h)_{\Omega_h^n} - \left(\psi'(Q^n), P_h^\ell\right)_{\Omega^n}}_{=:\eta^2 \widetilde{\mathcal{E}_\psi}(P_h)}.$$

Next, we use a change of variables and the mean value theorem for integrals with $c_1 \in [0,1]$:

$$\begin{aligned}
\left|\eta^2 \widetilde{\mathcal{E}_\psi}(P_h)\right| &\le \left| \int_{\Omega_h^n} \psi''(c_1 Q_I^n + (1-c_1)Q^n)(Q_I^n - Q^n) : P_h d\boldsymbol{x} \right| \\
&+ \left| \int_{\Omega_h^n} [\psi'(Q^n) - \psi'(Q^n)\circ \boldsymbol{\Phi}] : P_h d\boldsymbol{x} \right| + \left| \int_{\Omega_h^n} \psi'(Q^n \circ \boldsymbol{\Phi}) : P_h[\det(\nabla \boldsymbol{\Phi}) - 1] d\boldsymbol{x} \right| \\
&\lesssim \left| \int_{\Omega_h^n} \psi''(c_1 Q_I^n + (1-c_1)Q^n)(Q_I^n - Q^n) : P_h d\boldsymbol{x} \right| \\
&+ \left| \int_{\Omega_h^n} \psi''(c_2 Q^n + (1-c_2)Q^n \circ \boldsymbol{\Phi})(Q^n - Q^n \circ \boldsymbol{\Phi}) : P_h d\boldsymbol{x} \right| + h^q \|\psi'(Q^n \circ \boldsymbol{\Phi})\|_{L^2(\Omega_h^n)} \|P_h\|_{L^2(\Omega_h^n)},
\end{aligned}$$

where we used the geometry approximation and, again, the mean value theorem for integrals with $c_2 \in [0,1]$. Now, we take advantage of the regularity of Q^n, use a generalized Hölder's inequality, and invoke a Sobolev embedding theorem which says that $P_h \in H^1(\Omega_h^n) \implies P_h \in L^6(\Omega_h^n)$ for $\Omega_h^n \subset \mathbb{R}^3$. Thus, we get

$$\begin{aligned}
\left|\eta^2 \widetilde{\mathcal{E}_\psi}(P_h)\right| &\lesssim \|\psi''(c_1 Q_I^n + (1-c_1)Q^n)\|_{L^3(\Omega_h^n)} \|Q_I^n - Q^n\|_{L^2(\Omega_h^n)} \|P_h\|_{L^6(\Omega_h^n)} \\
&+ \|\psi''(c_2 Q^n + (1-c_2)Q^n \circ \boldsymbol{\Phi})\|_{L^3(\Omega_h^n)} \|Q^n - Q^n \circ \boldsymbol{\Phi}\|_{L^2(\Omega_h^n)} \|P_h\|_{L^6(\Omega_h^n)} \\
&+ h^q \left[\|Q^n\|_{L^6(\Omega_h^n)}^3 + \|Q^n\|_{L^4(\Omega_h^n)}^2 + \|Q^n\|_{L^2(\Omega_h^n)} \right] \|P_h\|_{L^2(\Omega_h^n)} \\
&\lesssim h^{m+1} \|Q^n\|_{H^{m+1}(\Omega_h^n)} \|P_h\|_{H^1(\Omega_h^n)} + h^{q+1} \|\nabla Q^n\|_{L^2(\Omega_h^n)} \|P_h\|_{H^1(\Omega_h^n)} + \widehat{C} h^q \|P_h\|_{L^2(\Omega_h^n)},
\end{aligned} \tag{106}$$

where the (implicit) constants in the inequality, and $\widehat{C} > 0$, depend on $\|Q^n\|_{H^2(\Omega_h^n)}$.

□

Lemma 9. *Assume $Q^n \in H^{m+1}(\Omega)$ for $m \ge 1$ and Assumption 1. Then, we have the following estimates:*

$$\begin{aligned}
\omega \mathcal{E}_\phi(P_h) &= (\phi'(Q_h^n) - \phi'(Q_I^n), P_h)_{\Gamma_h^n} + \omega \widetilde{\mathcal{E}_\phi}(P_h), \\
\left|\omega \widetilde{\mathcal{E}_\phi}(P_h)\right| &\lesssim \left[h^m \|Q^n\|_{H^{m+1}(\Omega_h^n)} + h^q \|\nabla Q^n\|_{H^2(\Omega_h^n)} + h^q \|Q^n\|_{H^1(\Omega_h^n)} \right] \|P_h\|_{H^1(\Omega_h^n)},
\end{aligned} \tag{107}$$

where the (implicit) constants in the inequality are independent of Q^n.

Proof. We first note the following identity:

$$\omega \mathcal{E}_\phi(P_h) = (\phi'(Q_h^n) - \phi'(Q_I^n), P_h)_{\Gamma_h^n} + \underbrace{(\phi'(Q_I^n), P_h)_{\Gamma_h^n} - \left(\phi'(Q^n), P_h^\ell\right)_{\Gamma^n}}_{=:\omega \widetilde{\mathcal{E}_\phi}(P_h)}.$$

Next, we use a change of variables and the mean value theorem for integrals with $c_1 \in [0,1]$:

$$\begin{aligned}
\left|\omega \widetilde{\mathcal{E}_\phi}(P_h)\right| &\le \left| \int_{\Gamma_h^n} \phi''(c_1 Q_I^n + (1-c_1)Q^n)(Q_I^n - Q^n) : P_h dS \right| \\
&+ \left| \int_{\Gamma_h^n} [\phi'(Q^n) - \phi'(Q^n)\circ \boldsymbol{\Phi}] : P_h dS \right| + \left| \int_{\Gamma_h^n} \phi'(Q^n \circ \boldsymbol{\Phi}) : P_h[\mu_h - 1] dS \right| \\
&\lesssim \left| \int_{\Gamma_h^n} \phi''(c_1 Q_I^n + (1-c_1)Q^n)(Q_I^n - Q^n) : P_h dS \right| \\
&+ \left| \int_{\Gamma_h^n} \phi''(c_2 Q^n + (1-c_2)Q^n \circ \boldsymbol{\Phi})(Q^n - Q^n \circ \boldsymbol{\Phi}) : P_h dS \right| + h^q \|\phi'(Q^n \circ \boldsymbol{\Phi})\|_{L^2(\Gamma_h^n)} \|P_h\|_{L^2(\Gamma_h^n)},
\end{aligned}$$

where we used the geometry approximation and, again, the mean value theorem for integrals with $c_2 \in [0,1]$.

Now, we take advantage of the regularity of Q^n and the fact that ϕ has quadratic growth and satisfies (10), i.e. $|\phi''(\cdot)|$ is bounded by a constant. Moreover, we use Cauchy-Schwarz, and invoke a standard trace theorem: $\|Q^n\|_{L^2(\Gamma_h^n)} \lesssim \|Q^n\|_{H^1(\Omega_h^n)}$. Thus, we get

$$\begin{aligned} \left|\omega\widetilde{\mathcal{E}_\phi}(P_h)\right| &\lesssim \left[\|Q_I^n - Q^n\|_{L^2(\Gamma_h^n)} + \|Q^n - Q^n \circ \mathbf{\Phi}\|_{L^2(\Gamma_h^n)} + h^q\|Q^n\|_{L^2(\Gamma_h^n)}\right] \|P_h\|_{L^2(\Gamma_h^n)} \\ &\lesssim \left[h^m\|Q^n\|_{H^{m+1}(\Omega_h^n)} + h^q\|\nabla Q^n\|_{H^2(\Omega_h^n)} + h^q\|Q^n\|_{H^1(\Omega_h^n)}\right] \|P_h\|_{H^1(\Omega_h^n)}, \end{aligned} \tag{108}$$

where the (implicit) constants in the inequality are independent of Q^n. □

We now prove the main consistency estimate using similar techniques as in Theorem 4 and the previous lemmas. In this case, the constant factor is exponential in the final time T.

Theorem 5 (Consistency Estimate)**.** *Assume $Q^n \in W^{2,\infty}(\mathcal{C}) \cap L^\infty([0,T]; H^{m+1}(\Omega(t)))$, $\partial_t Q^n \in L^\infty([0,T]; H^m(\Omega(t)))$, and Assumption 1. Then, we have the following:*

$$\begin{aligned} &\|\mathbb{E}^k\|^2_{L^2(\Omega_h^k)} + \frac{\alpha_1}{2}\triangle t \sum_{n=1}^{k} \|\mathbb{E}^n\|^2_{H^1(\Omega_h^n)} + \triangle t \gamma_{\mathrm{s}} \sum_{n=1}^{k} s_h^n\left(\mathbb{E}^n, \mathbb{E}^n\right) \\ &\qquad \leq \widetilde{Z}\left(4\theta_3 T \exp\left(2(C_2+\theta_2)T\right) \cdot (\triangle t + h^q + h^m)^2 + H_0 h^{2m}\right), \quad \text{for } k = 1, 2, ..., N, \end{aligned} \tag{109}$$

where θ_2, θ_3 depend on various constants in the problem (but not on the exact solution), $\widetilde{Z}$ depends on the exact solution and given data, and C_2 depends on the extension operator.

Proof. Recall (96) and test with $P_h = 2\triangle t e_h^n$

$$\begin{aligned} &2\int_{\Omega_h^n} (e_h^n - e_h^{n-1}) : e_h^n d\boldsymbol{x} + 2\triangle t a_h^n\left(e_h^n, e_h^n\right) + 2\gamma_{\mathrm{s}}\triangle t s_h(\mathcal{F}^n_{\Sigma_\delta^\pm}; e_h^n, e_h^n) \\ &\qquad = 2\triangle t\left[\mathcal{E}_I(e_h^n) + \mathcal{E}_0(e_h^n) + \mathcal{E}_B(e_h^n) + \mathcal{E}_\psi(e_h^n) + \mathcal{E}_\phi(e_h^n)\right], \end{aligned} \tag{110}$$

and note the following trivial relation:

$$\begin{aligned} 2\int_{\Omega_h^n} (e_h^n - e_h^{n-1}) : e_h^n d\boldsymbol{x} &= \|e_h^n\|^2_{L^2(\Omega_h^n)} - \|e_h^{n-1}\|^2_{L^2(\Omega_h^n)} + \int_{\Omega_h^n} e_h^n : e_h^n - 2e_h^n : e_h^{n-1} + e_h^{n-1} : e_h^{n-1} d\boldsymbol{x} \\ &= \|e_h^n\|^2_{L^2(\Omega_h^n)} - \|e_h^{n-1}\|^2_{L^2(\Omega_h^n)} + \|e_h^n - e_h^{n-1}\|^2_{L^2(\Omega_h^n)} \\ &\geq \|e_h^n\|^2_{L^2(\Omega_h^n)} - \|e_h^{n-1}\|^2_{L^2(\Omega_h^n)}. \end{aligned}$$

Then, using the discrete version of (36):

$$a_h^n\left(e_h^n, e_h^n\right) \geq \frac{\alpha_1}{2}\|e_h^n\|^2_{H^1(\Omega_h^n)} - \theta_1\|e_h^n\|^2_{L^2(\Omega_h^n)},$$

gives the following:

$$(1 - 2\theta_1\triangle t)\|e_h^n\|^2_{L^2(\Omega_h^n)} + \alpha_1\triangle t\|e_h^n\|^2_{H^1(\Omega_h^n)} + 2\gamma_{\mathrm{s}}\triangle t s_h^n\left(e_h^n, e_h^n\right) \leq 2\triangle t\mathcal{E}^n + \|e_h^{n-1}\|^2_{L^2(\Omega_h^n)}, \tag{111}$$

where $\mathcal{E}^n := \mathcal{E}_I(e_h^n) + \mathcal{E}_0(e_h^n) + \mathcal{E}_B(e_h^n) + \mathcal{E}_\psi(e_h^n) + \mathcal{E}_\phi(e_h^n)$.

Next, we note several estimates for the terms in $\mathcal{E}^n$. From Lemma 5, we have

$$|\mathcal{E}_I(e_h^n)| \lesssim \frac{\gamma_I}{2}h^{2m}KR_I(Q) + \frac{1}{2\gamma_I}\left[\|e_h^n\|^2_{H^1(\Omega_h^n)} + s_h^n\left(e_h^n, e_h^n\right)\right], \tag{112}$$

for any $\gamma_I > 0$, where $R_I(Q)$ depends on the exact solution Q. From Lemma 6,

$$|\mathcal{E}_0(e_h^n)| \lesssim \frac{\gamma_0}{2}\left(\triangle t + h^q + h^m\right)^2 R_0^2(Q, \mathbf{v}, U_\Omega, Q_\Gamma) + \frac{1}{2\gamma_0}\left[\|e_h^n\|^2_{H^1(\Omega_h^n)} + s_h^n\left(e_h^n, e_h^n\right)\right], \tag{113}$$

for any $\gamma_0 > 0$, where R_0 depends on the exact solution and the given data. For the Beris-Edwards term, Lemma 7 gives

$$|\mathcal{E}_B(e_h^n)| \lesssim \frac{\gamma_B}{2}(h^{m+1} + h^q)^2 R_B^2 + \frac{1}{2\gamma_B}\|e_h^n\|_{H^1(\Omega_h^n)}^2, \tag{114}$$

for any $\gamma_B > 0$, where R_B depends on the exact solution and given data. Next, we note the estimates for the double-well terms. For the bulk potential, Lemma 8 gives

$$\mathcal{E}_\psi(e_h^n) = -\eta^{-2}\left(\psi'(Q_I^n) - \psi'(Q_h^n), e_h^n\right)_{\Omega_h^n} + \widetilde{\mathcal{E}_\psi}(e_h^n) \le -\eta^{-2}\left(\psi_e'(Q_I^n) - \psi_e'(Q_h^n), e_h^n\right)_{\Omega_h^n} + \widetilde{\mathcal{E}_\psi}(e_h^n),$$

where we used the convex-splitting and convexity of ψ_c. Thus, we get

$$|\mathcal{E}_\psi(e_h^n)| \lesssim \frac{1}{\eta^2}\left[\beta_\psi\|e_h^n\|_{L^2(\Omega_h^n)}^2 + \frac{\gamma_\psi}{2}(h^{m+1} + h^q)^2 R_\psi^2(Q) + \frac{1}{2\gamma_\psi}\|e_h^n\|_{H^1(\Omega_h^n)}^2\right], \tag{115}$$

for any $\gamma_\psi > 0$, where R_ψ depends on the exact solution. Similarly, for the boundary potential, Lemma 9 gives

$$|\mathcal{E}_\phi(e_h^n)| \lesssim \frac{1}{\omega}\left[\frac{\gamma_\phi}{2}\beta_\phi^2\|e_h^n\|_{L^2(\Omega_h^n)}^2 + \frac{\gamma_\phi}{2}(h^m + h^q)^2 R_\phi^2(Q) + \frac{1}{\gamma_\phi}\|e_h^n\|_{H^1(\Omega_h^n)}^2\right], \tag{116}$$

for any $\gamma_\phi > 0$, where R_ϕ depends on the exact solution.

Then, choosing γ_I, γ_0, γ_B, γ_ψ, γ_ϕ appropriately, and plugging into (111), we arrive at

$$\begin{aligned}(1 - \triangle t\theta_2)\|e_h^n\|_{L^2(\Omega_h^n)}^2 + \frac{\alpha_1}{2}\triangle t\|e_h^n\|_{H^1(\Omega_h^n)}^2 + \gamma_{\mathrm{s}}\triangle t s_h^n\left(e_h^n, e_h^n\right) \\ \le \|e_h^{n-1}\|_{L^2(\Omega_h^n)}^2 + \theta_3\widetilde{R}\triangle t\left(\triangle t + h^q + h^m\right)^2,\end{aligned} \tag{117}$$

where θ_2, θ_3 depend on various constants in the problem (but not on the exact solution), and $\widetilde{R}$ depends on the exact solution and the given data.

Now, we use (17), and apply Lemma 3 componentwise, to get the following estimates for $\|e_h^{n-1}\|_{L^2(\Omega_h^n)}^2$ that hold for all $1 \le n \le N$ for constants C_1, C_2, C_3 that do not depend on n:

$$\begin{aligned}\|e_h^0\|_{L^2(\Omega_h^1)}^2 &\le \|e_h^0\|_{L^2(\mathcal{O}_\delta(\Omega_h^0))}^2 \le C_1\|e_h^0\|_{L^2(\Omega_h^0)}^2 + C_1Kh^2 s_h^0(e_h^0, e_h^0), \\ \|e_h^{n-1}\|_{L^2(\Omega_h^n)}^2 &\le \|e_h^{n-1}\|_{L^2(\mathcal{O}_\delta(\Omega_h^{n-1}))}^2 \\ &\le (1 + C_2\triangle t)\|e_h^{n-1}\|_{L^2(\Omega_h^{n-1})}^2 + \frac{\alpha_1}{4}\triangle t\|\nabla e_h^{n-1}\|_{L^2(\Omega_h^{n-1})}^2 + C_3\triangle tKs_h^{n-1}(e_h^{n-1}, e_h^{n-1}).\end{aligned} \tag{118}$$

Now, by summing up (117) over $n = 1, ..., k$, we get the following:

$$\begin{aligned}(1 - \triangle t\theta_2)\sum_{n=1}^{k}\|e_h^n\|_{L^2(\Omega_h^n)}^2 + \frac{\alpha_1}{2}\triangle t\sum_{n=1}^{k}\|e_h^n\|_{H^1(\Omega_h^n)}^2 + \triangle t\gamma_{\mathrm{s}}\sum_{n=1}^{k}s_h^n\left(e_h^n, e_h^n\right) \\ \le \sum_{n=1}^{k}\|e_h^{n-1}\|_{L^2(\Omega_h^n)}^2 + \theta_3\widetilde{R}\left(\triangle t + h^q + h^m\right)^2\sum_{n=1}^{N}\triangle t.\end{aligned} \tag{119}$$

Then, by applying (118) and choosing $\gamma_{\mathrm{s}} \ge 2C_3K$, we get

$$\begin{aligned}&(1 - \triangle t\theta_2)\|e_h^k\|_{L^2(\Omega_h^k)}^2 + \frac{\alpha_1}{4}\triangle t\sum_{n=1}^{k}\|e_h^n\|_{H^1(\Omega_h^n)}^2 + \triangle t\frac{\gamma_{\mathrm{s}}}{2}\sum_{n=1}^{k}s_h^n\left(e_h^n, e_h^n\right) \\ &\le \theta_3\widetilde{R}T\left(\triangle t + h^q + h^m\right)^2 + C_1\|e_h^0\|_{L^2(\Omega_h^0)}^2 + C_1Kh^2 s_h^0(e_h^0, e_h^0) + \triangle t\sum_{n=2}^{k}(C_2 + \theta_2)\|e_h^{n-1}\|_{L^2(\Omega_h^{n-1})}^2.\end{aligned} \tag{120}$$

Now, choose $\triangle t\theta_2 < \frac{1}{2}$ and note that $e_h^0 = 0$ on $\mathcal{O}_\delta(\Omega_h^n)$ to obtain

$$\begin{aligned}\|e_h^k\|^2_{L^2(\Omega_h^k)} + \frac{\alpha_1}{2}\triangle t\sum_{n=1}^{k}\|e_h^n\|^2_{H^1(\Omega_h^n)} + \triangle t\gamma_{\mathrm{s}}\sum_{n=1}^{k}s_h^n\left(e_h^n, e_h^n\right) \\ \leq 2\theta_3\widetilde{R}T\left(\triangle t + h^q + h^m\right)^2 + \triangle t\sum_{n=1}^{k-1}2(C_2+\theta_2)\|e_h^n\|^2_{L^2(\Omega_h^n)}.\end{aligned} \tag{121}$$

Now, by the discrete Grönwall inequality stated in Lemma 14 of the appendix, we get the following:

$$\begin{aligned}\|e_h^k\|^2_{L^2(\Omega_h^k)} + \frac{\alpha_1}{2}\triangle t\sum_{n=1}^{k}\|e_h^n\|^2_{H^1(\Omega_h^n)} + \triangle t\gamma_{\mathrm{s}}\sum_{n=1}^{k}s_h^n\left(e_h^n, e_h^n\right) \\ \leq 2\theta_3\widetilde{R}T\exp\left(2(C_2+\theta_2)T\right)\cdot\left(\triangle t + h^q + h^m\right)^2.\end{aligned} \tag{122}$$

Then, by using a triangle inequality with a standard interpolation result we get

$$\begin{aligned}&\|\mathbb{E}^k\|^2_{L^2(\Omega_h^k)} + \frac{\alpha_1}{2}\triangle t\sum_{n=1}^{k}\|\mathbb{E}^n\|^2_{H^1(\Omega_h^n)} + \triangle t\gamma_{\mathrm{s}}\sum_{n=1}^{k}s_h^n\left(\mathbb{E}^n, \mathbb{E}^n\right) \\ &\quad\leq 4\theta_3\widetilde{R}T\exp\left(2(C_2+\theta_2)T\right)\cdot\left(\triangle t + h^q + h^m\right)^2 \\ &\qquad + 2\|e^k\|^2_{L^2(\Omega^k)} + \alpha_1\triangle t\sum_{n=1}^{k}\|e^n\|^2_{H^1(\Omega_h^n)} + 2\triangle t\gamma_{\mathrm{s}}\sum_{n=1}^{k}s_h^n\left(e^n, e^n\right) \\ &\quad\leq 4\theta_3\widetilde{R}T\exp\left(2(C_2+\theta_2)T\right)\cdot\left(\triangle t + h^q + h^m\right)^2 + H_0\sup_{t\in[0,T]}\|Q\|^2_{H^{m+1}(\Omega(t))}h^{2m},\end{aligned}$$

for some independent constant H_0, which delivers (109). □

6 Numerical Results

We present simulations with different choices of anchoring conditions that depict how LC defects are induced by the colloidal objects as well as the interaction of the colloids with the surrounding LC medium. See [7, 46, 26] for an explanation of defects in LCs. All simulations were implemented in `NGSolve` [41] with the add-on package `ngsxfem` for unfitted methods [33]. We use a standard Newton-scheme to solve the non-linear system at each time-step. The hardware used for the simulations was the following laptop: Lenovo ThinkPad P14s Gen 5, Intel(R) Core(TM) Ultra 7 155H, 1400 Mhz, 16 Cores, 22 Logical Processors, 96 GB of RAM.

6.1 Convergence Check

The box domain is taken to be $\widehat{\mathfrak{D}} = [0,1]^2$ in two dimensions and is triangulated with a uniform mesh of size $h = h_0 2^{-k}$, where $h_0 = 0.1$ and $k \geq 0$ is the refinement level. The LC domain is defined by $\Omega(t) = \widehat{\mathfrak{D}} \setminus D(t)$, where $D(t)$ denotes the domain of a moving colloid whose path is parameterized by

$$x(t) = 0.5 + 0.15\sin((\pi/8)t), \quad y(t) = 0.5 + 0.15\cos((\pi/2)t), \tag{123}$$

where $(x(t), y(t))$ refers to the center of the colloid, which is a disk of radius 0.2. Time-dependent level set functions are used to track the domain $\Omega(t)$ using $\mathcal{P}_2$ Lagrange elements.

With the velocity of the colloid known, we compute the fluid velocity $\mathbf{v}$ in Ω by solving a Stokes problem using an unfitted method [25, 35, 32, 50]. We use $\mathcal{P}_2$-$\mathcal{P}_1$ Taylor-Hood elements for velocity and pressure with the following stabilization parameters

$$\gamma_{\mathrm{vel}} = 0.05, \quad \gamma_{\mathrm{p}} = 0.05, \quad \gamma_{\mathrm{D}} = 150. \tag{124}$$

The time interval is taken to be $[0, T]$ with $T = 2.0$ and $N = 10 \cdot 2^k$ time steps. The elastic coefficients are given by $\ell_1 = 1.0$, $\ell_2 = 0.5$, $\ell_3 = 0.4$. The bulk potential is given by (6) with constants:

$$a_0 = 1.0, \quad a_2 = 16.3265, \quad a_3 = 0.0, \quad a_4 = 66.6389. \tag{125}$$

and bulk constant: $\eta = 1.0$. Note that $\psi(Q)$ achieves its global minimum of 0.0 when Q has the form of (2) with s replaced by $s_0 = 0.7$. The weak anchoring constants are chosen to be

$$w_0 = 1.0, \quad w_1 = 1.0, \quad 1/\omega = 1.0, \tag{126}$$

and the Beris–Edwards parameter is $p_0 = 0.5$.

Our numerical scheme uses $\mathcal{P}_2$ Lagrange elements for approximating Q with the following unfitted parameters defined similar to [34]:

$$\delta = 1.2 \triangle t \mathbf{v}_\infty^n, \quad \widetilde{K} = \operatorname{int}\left(1 + \operatorname{ceil}(\delta/h)\right), \quad \gamma_{\mathrm{s}} = c_\gamma \widetilde{K}, \quad c_\gamma = 1.1, \tag{127}$$

where $\mathbf{v}_\infty^n$ is computed from the known colloid velocity.

Since we are in two dimensions, there are two symmetric traceless, orthonormal basis matrices $\{E^1, E^2\}$ that span $\mathbf{S}_0$ which are given by

$$E^1 = \begin{bmatrix} 1/\sqrt{2} & 0 \\ 0 & -1/\sqrt{2} \end{bmatrix}, \quad E^2 = \begin{bmatrix} 0 & 1/\sqrt{2} \\ 1/\sqrt{2} & 0 \end{bmatrix}.$$

The exact solution is then chosen to be

$$Q(t, x_1, x_2) = \cos(t) \left[\sin(2\pi x_1) E^1 + \cos(2\pi x_2) E^2\right], \tag{128}$$

and we compute U_Ω such that (128) exactly solves (14); note: we include an extra "right-hand-side" term in the boundary condition in (14) to fit the manufactured solution. A strong anchoring condition is given on the outer boundary of the box $\partial\widehat{\mathfrak{D}}$: $Q = Q_{\mathrm{D}}$ which matches (128); similarly, the initial condition matches (128).

Referring to the error estimate in (109), we have $q = 2$, $m = 2$. The convergence results are given in Table 1. Note that the convergence rate is limited by the first order time-discretization error.

k	$L^2(0,T;L^2(\Omega(t)))$	$L^\infty(0,T;L^2(\Omega(t)))$	$L^2(0,T;H^1(\Omega(t)))$
0	1.7411E-03 (—)	1.7630E-03 (—)	5.9067E-02 (—)
1	2.4378E-04 (2.84)	2.0153E-04 (3.129)	1.2572E-02 (2.232)
2	9.8959E-05 (1.30)	8.2683E-05 (1.285)	3.2733E-03 (1.941)
3	4.8485E-05 (1.03)	4.1277E-05 (1.002)	9.5014E-04 (1.785)

Table 1: Convergence results for the exact solution in (128). The mesh size is $h = h_0 2^{-k}$ (where $h_0 = 0.1$), the time step is $\triangle t = \triangle t_0 2^{-k}$ (where $\triangle t_0 = 0.2$), and $k \geq 0$ is the refinement level. The experimental order of convergence is given in parenthesis.

6.2 Two Colloids Moving Vertically

The box domain is taken to be $\widehat{\mathfrak{D}} = [0, 1.5] \times [0, 1]$ in two dimensions and is triangulated with a uniform mesh of size $h = 0.05$. The LC domain is defined by $\Omega(t) = \widehat{\mathfrak{D}} \setminus (D_1(t) \cup D_2(t))$, where $D_i(t)$ denotes the domain of the i-th moving colloid. The two colloids have paths parameterized by

$$\begin{aligned} x_1(t) &= 0.4, \quad y_1(t) = 0.5 + 0.2\sin((\pi/4)t), \\ x_2(t) &= 1.1, \quad y_2(t) = 0.5 - 0.2\sin((\pi/4)t), \end{aligned} \tag{129}$$

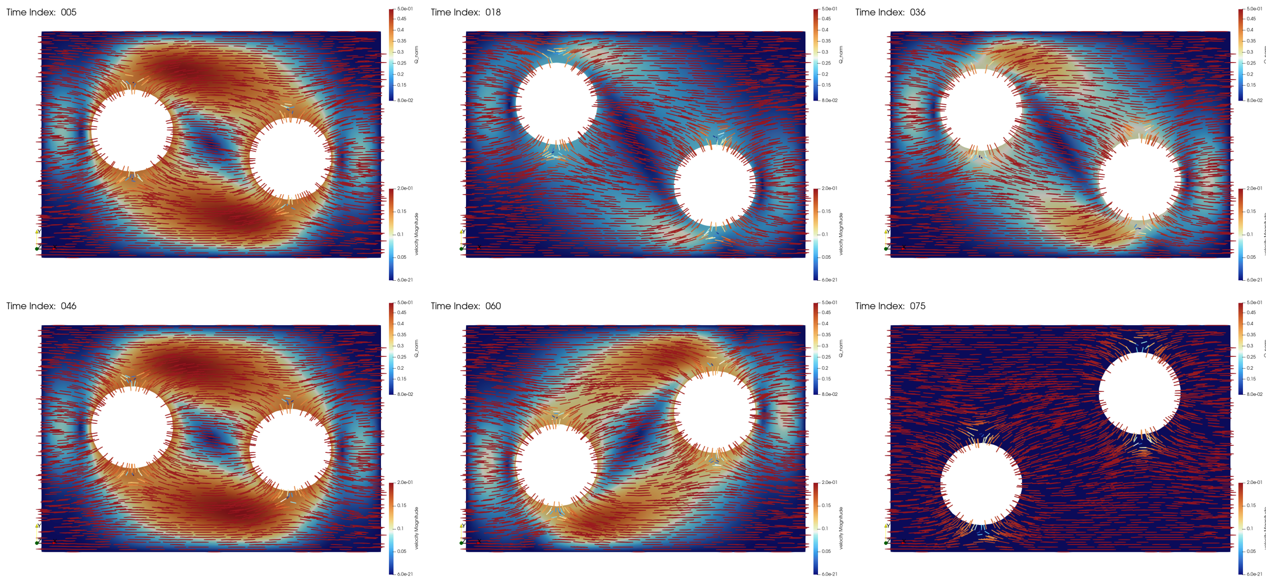

Figure 2: Two colloids moving vertically with normal anchoring (Section 6.2). The line segments depict the director $\mathbf{n}$ of the liquid crystal which is the dominant eigenvector of Q (color is $|Q|$). The background color is $|\mathbf{v}|$. Two $-1/2$ defects are located near the vertical poles of each colloid.

where $(x_i(t), y_i(t))$ refers to the center of the i-th colloid, which is a disk of radius 0.18. Time-dependent level set functions are used to track the domain $\Omega(t)$ using $\mathcal{P}_2$ Lagrange elements.

With the velocity of each colloid known, we compute the fluid velocity $\mathbf{v}$ in Ω by solving a Stokes problem using an unfitted method as described in Section 6.1. The time interval is taken to be $[0, T]$ with $T = 16.0$ using $N = 200$. The elastic coefficients are given by $\ell_1 = 1.0$, $\ell_2 = 0.0$, $\ell_3 = 0.0$. The bulk potential $\psi(Q)$ is given by (6) with constants given in (125) and bulk coefficient: $\eta = 0.1$. Note that $\psi(Q)$ achieves its global minimum of 0.0 when Q has the form of (2) with s replaced by $s_0 = 0.7$.

The weak anchoring constants are either of two choices:

$$\begin{aligned} \text{Normal Anchoring:} &\quad w_0 = 100, \quad w_1 = 0, \quad 1/\omega = 0, \\ \text{Planar Anchoring:} &\quad w_0 = 0, \quad w_1 = 100, \quad 1/\omega = 100. \end{aligned} \tag{130}$$

The Beris–Edwards parameter $p_0 = 0.0$. Our numerical scheme uses $\mathcal{P}_2$ Lagrange elements for approximating Q with unfitted parameters defined as in (127).

A strong anchoring condition is given on the outer boundary of the box $\partial\widehat{\mathfrak{D}}$: $Q = Q_{\mathrm{D}}$ with

$$Q_{\mathrm{D}} = s_0 \left(\mathbf{e}_1 \otimes \mathbf{e}_1 - \frac{1}{2} I \right), \tag{131}$$

where $\mathbf{e}_1 = (1, 0)$. The initial condition is given by

$$Q_0 = s_0 \left(\mathbf{e}_2 \otimes \mathbf{e}_2 - \frac{1}{2} I \right), \tag{132}$$

where $\mathbf{e}_2 = (0, 1)$.

Figure 2 shows snapshots of the simulation with normal anchoring. The liquid crystal director $\mathbf{n}$ (i.e. the dominant eigenvector of Q) is orthogonal to the colloid surfaces; $\mathbf{n}$ is aligned with $\mathbf{e}_1$ on $\partial\widehat{\mathfrak{D}}$. One can see how $\mathbf{n}$ is affected by the relative position of the colloids. Furthermore, two $-1/2$ defects are at opposite ends of each colloid which follow the motion of the colloids. The effect of the initial condition is heavily damped out because of the high anchoring coefficients and the small value of $\eta = 0.1$.

Figure 3 shows snapshots of the simulation with planar anchoring. The liquid crystal director $\mathbf{n}$ is parallel to the colloid surfaces; $\mathbf{n}$ is aligned with $\mathbf{e}_1$ on $\partial\widehat{\mathfrak{D}}$. The alignment of the director in the center of the domain

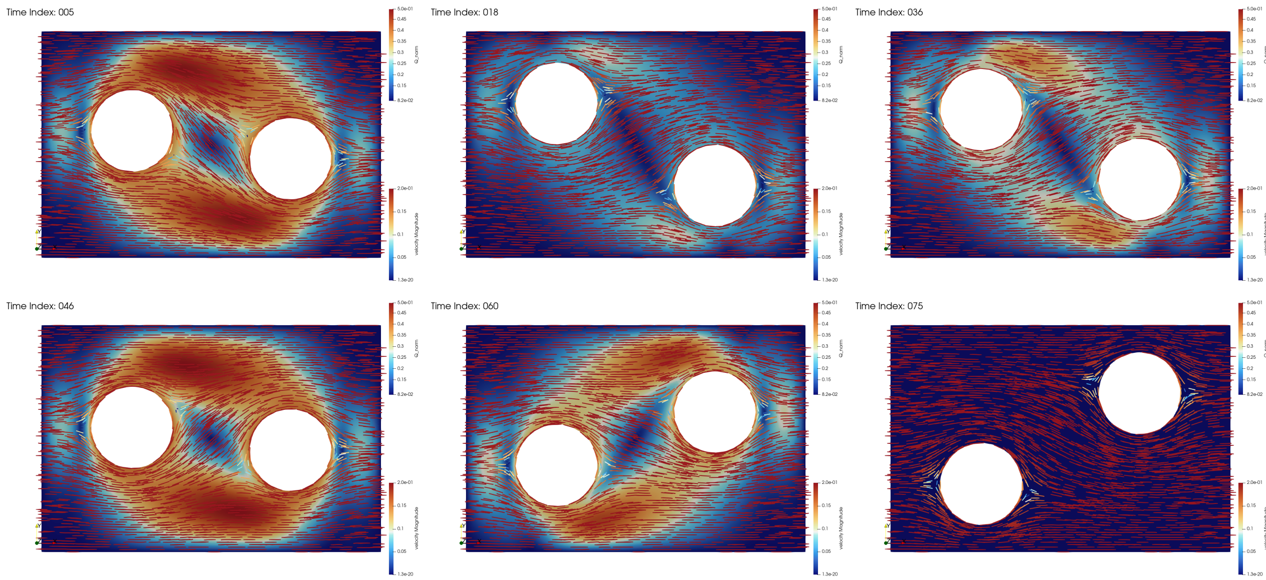

Figure 3: Two colloids moving vertically with planar anchoring (Section 6.2). The line segments depict the director $\mathbf{n}$ of the liquid crystal which is the dominant eigenvector of Q (color is $|Q|$). The background color is $|\mathbf{v}|$. Two $-1/2$ defects are located near the horizontal poles of each colloid.

"switches" between two distinct directions as the colloids move back and forth. Furthermore, two $-1/2$ defects are at opposite ends of each colloid which follow the motion of the colloids. The effect of the initial condition is heavily damped out here as well.

6.3 Two Colloids Moving Horizontally

The box domain is taken to be $\widehat{\mathfrak{D}} = [0, 1.5] \times [0, 1]$ in two dimensions and is triangulated with a uniform mesh of size $h = 0.05$. The LC domain is defined by $\Omega(t) = \widehat{\mathfrak{D}} \setminus (D_1(t) \cup D_2(t))$, where $D_i(t)$ denotes the domain of the i-th moving colloid. The two colloids have paths parameterized by

$$\begin{aligned} x_1(t) &= 0.75 + 0.4\sin((\pi/4)t), \quad y_1(t) = 0.75, \\ x_2(t) &= 0.75 - 0.4\sin((\pi/4)t), \quad y_2(t) = 0.25, \end{aligned} \tag{133}$$

where $(x_i(t), y_i(t))$ refers to the center of the i-th colloid, which is a disk of radius 0.15. Time-dependent level set functions are used to track the domain $\Omega(t)$ using $\mathcal{P}_2$ Lagrange elements.

With the velocity of each colloid known, we compute the fluid velocity $\mathbf{v}$ in Ω by solving a Stokes problem using an unfitted method as described in Section 6.1. The time interval is taken to be $[0, T]$ with $T = 16.0$ using $N = 400$. The elastic coefficients are given by $\ell_1 = 1.0$, $\ell_2 = 0.0$, $\ell_3 = 0.0$. The bulk potential $\psi(Q)$ is given by (6) with constants given in (125) and bulk coefficient: $\eta = 0.1$. Note that $\psi(Q)$ achieves its global minimum of 0.0 when Q has the form of (2) with s replaced by $s_0 = 0.7$.

The weak anchoring constants are either of two choices:

$$\begin{aligned} \text{Normal Anchoring:} \quad & w_0 = 100, \quad w_1 = 0, \quad 1/\omega = 0, \\ \text{Planar Anchoring:} \quad & w_0 = 0, \quad w_1 = 100, \quad 1/\omega = 100. \end{aligned} \tag{134}$$

The Beris–Edwards parameter $p_0 = 0.0$. Our numerical scheme uses $\mathcal{P}_2$ Lagrange elements for approximating Q with unfitted parameters defined as in (127).

A strong anchoring condition is given on the outer boundary of the box $\partial\widehat{\mathfrak{D}}$, $Q = Q_{\mathrm{D}}$, using (131). The initial condition is given by (132).

Figure 4 shows snapshots of the simulation with normal anchoring. The liquid crystal director $\mathbf{n}$ (i.e. the dominant eigenvector of Q) is orthogonal to the colloid surfaces; $\mathbf{n}$ is aligned with $\mathbf{e}_1$ on $\partial\widehat{\mathfrak{D}}$. One can see how

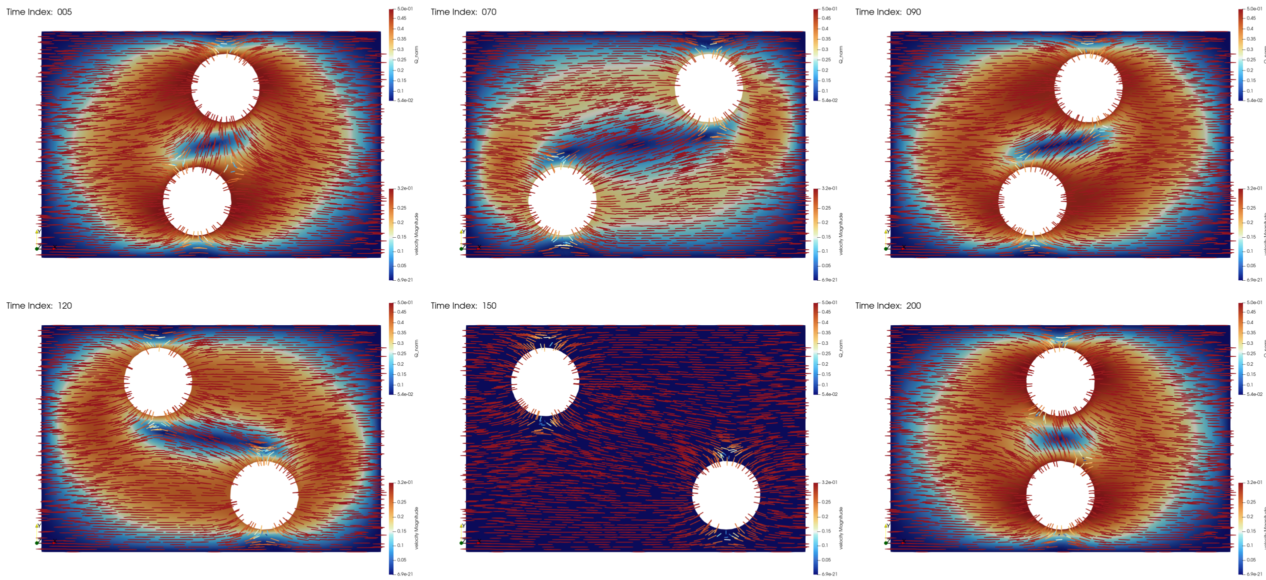

Figure 4: Two colloids moving horizontally with normal anchoring (Section 6.3). Same format as Figure 2. Two $-1/2$ defects are located near the vertical poles of each colloid.

$\mathbf{n}$ is affected by the relative position of the colloids. The alignment of $\mathbf{n}$ in the center of the domain switches between two main orientations as the two colloids pass each other.

Furthermore, each colloid has two $-1/2$ defects that mainly hover near opposite poles of the colloid as it moves. However, there is some variation here. In the top-left plot, the top colloid "loses" its bottom defect to the bottom colloid (i.e. the bottom colloid has three $-1/2$ defects). In addition, the bottom-right plot shows that the defects are not at opposite poles, but slightly displaced. The effect of the initial condition is heavily damped out because of the high anchoring coefficients and the small value of $\eta = 0.1$.

Figure 5 shows snapshots of the simulation with planar anchoring. The liquid crystal director $\mathbf{n}$ is parallel to the colloid surfaces; $\mathbf{n}$ is aligned with $\mathbf{e}_1$ on $\partial\widehat{\mathfrak{D}}$. The alignment of the director in the center of the domain smoothly varies as the colloids move back and forth. Furthermore, two $-1/2$ defects are at opposite ends of each colloid which follow the motion of the colloids. The effect of the initial condition is heavily damped out here as well.

6.4 Two Colloids Moving in a Circle

The box domain is taken to be $\widehat{\mathfrak{D}} = [0, 1.5]^2$ in two dimensions and is triangulated with a uniform mesh of size $h = 0.05$. The LC domain is defined by $\Omega(t) = \widehat{\mathfrak{D}} \setminus (D_1(t) \cup D_2(t))$, where $D_i(t)$ denotes the domain of the i-th moving colloid. The two colloids have paths parameterized by

$$\begin{aligned} x_1(t) &= 0.75 + 0.4\cos((\pi/4)t), \quad y_1(t) = 0.75 + 0.4\sin((\pi/4)t), \\ x_2(t) &= 0.75 - 0.4\cos((\pi/4)t), \quad y_2(t) = 0.75 - 0.4\sin((\pi/4)t), \end{aligned} \tag{135}$$

where $(x_i(t), y_i(t))$ refers to the center of the i-th colloid, which is a disk of radius 0.2. Time-dependent level set functions are used to track the domain $\Omega(t)$ using $\mathcal{P}_2$ Lagrange elements.

With the velocity of each colloid known, we compute the fluid velocity $\mathbf{v}$ in Ω by solving a Stokes problem using an unfitted method as described in Section 6.1. The time interval is taken to be $[0, T]$ with $T = 16.0$ using $N = 400$. The elastic coefficients are given by $\ell_1 = 1.0$, $\ell_2 = 0.0$, $\ell_3 = 0.0$. The bulk potential $\psi(Q)$ is given by (6) with constants given in (125) and bulk coefficient: $\eta = 0.1$. Note that $\psi(Q)$ achieves its global minimum of 0.0 when Q has the form of (2) with s replaced by $s_0 = 0.7$.

The weak anchoring constants are either of two choices:

$$\begin{aligned} \text{Normal Anchoring:} \quad & w_0 = 100, \quad w_1 = 0, \quad 1/\omega = 0, \\ \text{Planar Anchoring:} \quad & w_0 = 0, \quad w_1 = 100, \quad 1/\omega = 100. \end{aligned} \tag{136}$$

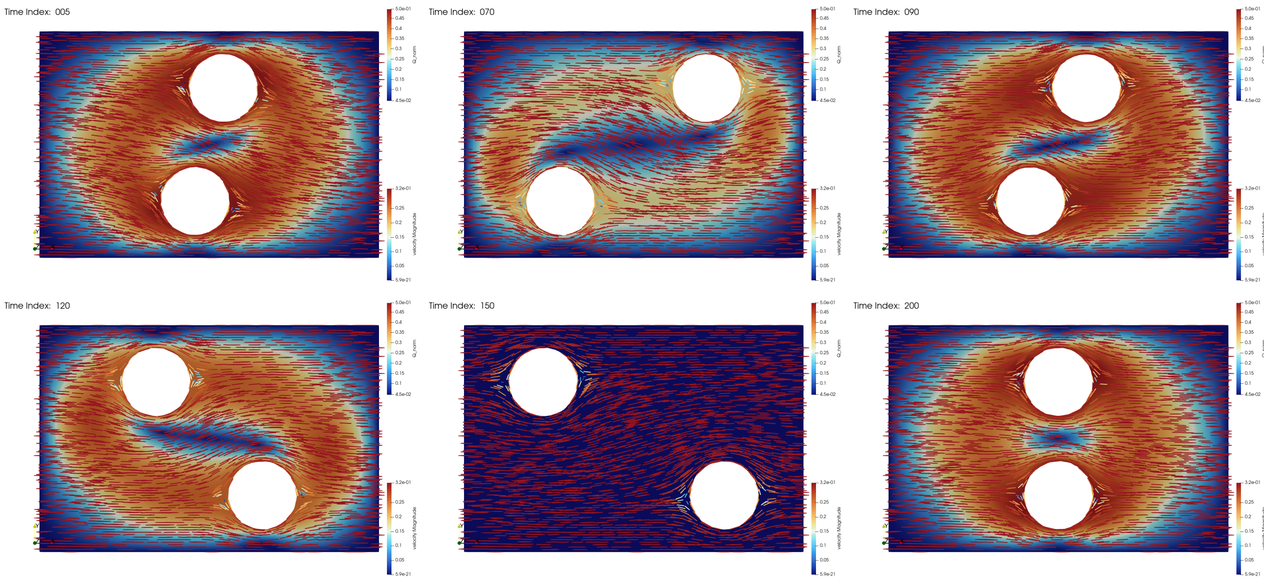

Figure 5: Two colloids moving horizontally with planar anchoring (Section 6.3). Same format as Figure 3. Two $-1/2$ defects are located near the horizontal poles of each colloid.

The Beris–Edwards parameter $p_0 = 0.0$. Our numerical scheme uses $\mathcal{P}_2$ Lagrange elements for approximating Q with unfitted parameters defined as in (127).

A strong anchoring condition is given on the outer boundary of the box $\partial\widehat{\mathfrak{D}}$, $Q = Q_{\mathrm{D}}$, using (131). The initial condition is given by (132).

Figure 6 shows snapshots of the simulation with normal anchoring. The liquid crystal director $\mathbf{n}$ (i.e. the dominant eigenvector of Q) is orthogonal to the colloid surfaces; $\mathbf{n}$ is aligned with $\mathbf{e}_1$ on $\partial\widehat{\mathfrak{D}}$. One can see how $\mathbf{n}$ is affected by the relative position of the colloids. The alignment of $\mathbf{n}$ in the center of the domain is fairly stable except for a sudden transition between time indices 60 and 75 where there is an abrupt change in orientation. Moreover, each colloid has two $-1/2$ defects that mainly hover near opposite poles of the colloid as it moves with some slight distortions. The effect of the initial condition is heavily damped out because of the high anchoring coefficients and the small value of $\eta = 0.1$.

Figure 7 shows snapshots of the simulation with normal anchoring. The liquid crystal director $\mathbf{n}$ (i.e. the dominant eigenvector of Q) is orthogonal to the colloid surfaces; $\mathbf{n}$ is aligned with $\mathbf{e}_1$ on $\partial\widehat{\mathfrak{D}}$. One can see how $\mathbf{n}$ is affected by the relative position of the colloids. The alignment of $\mathbf{n}$ in the center of the domain smoothly varies except for a sudden transition between time indices 115 and 125 where there is an abrupt change in orientation. Also, the liquid crystal state is different for time indices 5 and 205, even though the colloids are in the exact same position. Moreover, each colloid has two $-1/2$ defects that mainly hover near opposite poles of the colloid as it moves with some mild distortions. The effect of the initial condition is heavily damped out because of the high anchoring coefficients and the small value of $\eta = 0.1$.

7 Remarks

We presented an unfitted finite element method to simulate LCs in moving domains based on a dynamic Landau–de Gennes model. Full convergence of the scheme is established with reasonable assumptions on the geometry. Our results highlight the potential of unfitted FEMs for simulating materials with embedded microstructures and can provide insight into the interplay between geometry, topology, and elasticity in liquid crystal–colloid systems.

Future extensions of this work would be to couple Stokes to the Dynamic Q-equation; some PDE theory is already available in [39]. In [20], they consider the problem of a moving colloid in a nematic LC. However, the main difficulty here is in extending unfitted FEM techniques to problems where the domain motion is part

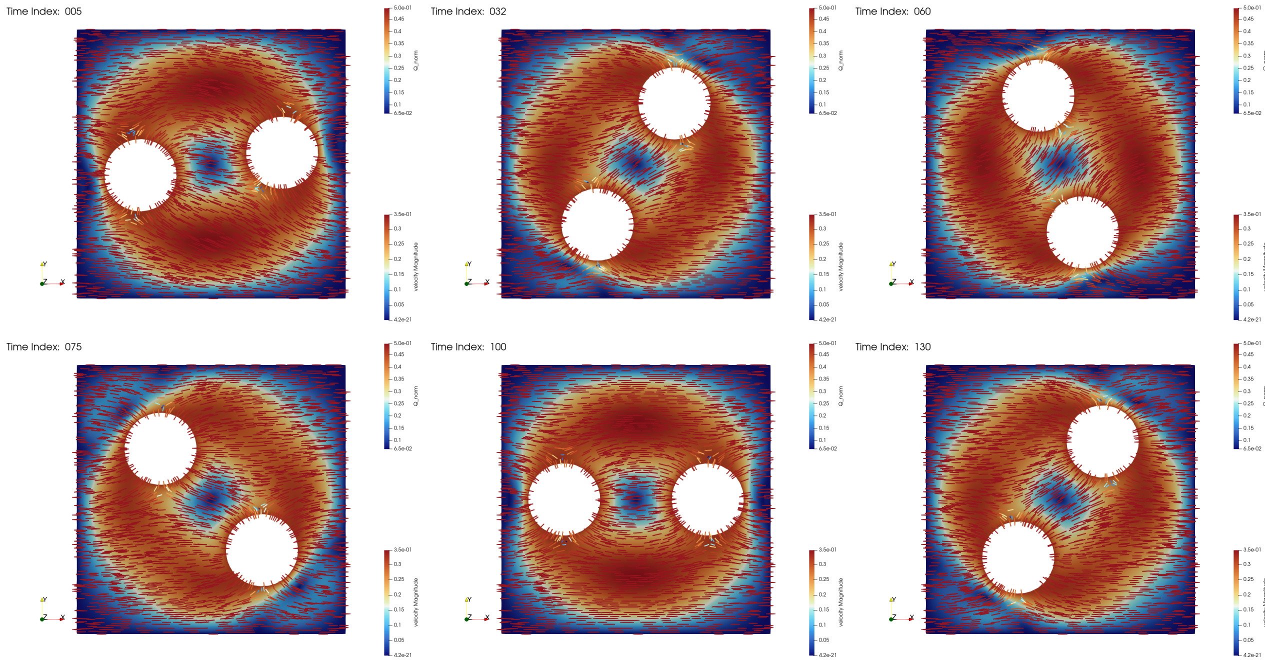

Figure 6: Two colloids moving in a circle with normal anchoring (Section 6.4). Same format as Figure 2. Two $-1/2$ defects are located near the vertical poles of each colloid.

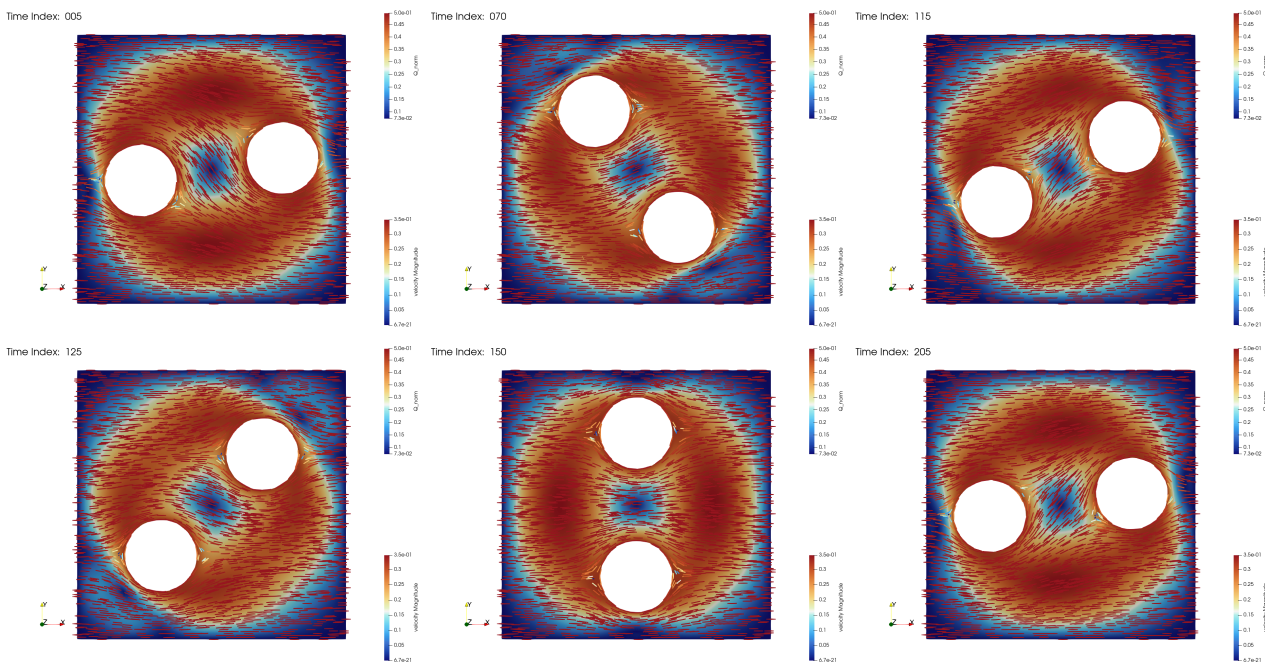

Figure 7: Two colloids moving horizontally with planar anchoring (Section 6.4). Same format as Figure 3. Two $-1/2$ defects are located near the horizontal poles of each colloid.

of the solution. As of this time, little work has been done in this area.

A Appendix

A.1 Extension Operator

The following is taken from Lemmas 3.4 and 3.5 in [34]. Given $y(t, \boldsymbol{x}) : \Omega(t) \to \mathbb{R}$, there exists an extension operator, denoted $\mathcal{E}$, such that

$$\mathcal{E}y(t, \boldsymbol{x}) : \mathcal{O}_\delta(\Omega(t)) \to \mathbb{R}, \tag{137}$$

where $\mathcal{E}$ has the following properties. For $y \in L^\infty([0,T]; H^{m+1}(\Omega(t))) \cap W^{2,\infty}(\Omega(t) \times [0,T])$ (see [34] for the function space definition) we have

$$\begin{aligned} \|\mathcal{E}y\|_{H^k(\mathcal{O}_\delta(\Omega(t)))} &\leq c_1 \|y\|_{H^k(\Omega(t))}, \quad k = 0, 1, ..., m+1 \\ \|\nabla(\mathcal{E}y)\|_{L^2(\mathcal{O}_\delta(\Omega(t)))} &\leq c_2 \|\nabla y\|_{L^2(\Omega(t))}, \\ \|\mathcal{E}y\|_{W^{2,\infty}(\mathcal{O}_\delta(\mathcal{C}))} &\leq c_3 \|y\|_{W^{2,\infty}(\mathcal{C})}, \end{aligned} \tag{138}$$

where the constants are independent of δ. Also, for $y \in L^\infty([0,T]; H^{m+1}(\Omega(t)))$ with $\partial_t y \in L^\infty([0,T]; H^m(\Omega(t)))$ we have

$$\|\partial_t(\mathcal{E}y)\|_{H^m(\mathcal{O}_\delta(\Omega(t)))} \leq c_4 \left(\|y\|_{H^{m+1}(\Omega(t))} + \|\partial_t y\|_{H^m(\Omega(t))} \right), \tag{139}$$

where c_4 does not depend on δ.

As for Q, we define its extension by $\mathcal{E}Q = (\mathcal{E}q_i)E^i$ which guarantees that the extension is traceless and satisfies similar estimates to (138), (139).

A.2 Geometric Approximation Estimates

Lemma 10. *Given $R \in L^q(\Omega_h^n)$, $S \in L^q(\Gamma_h^n)$, $T \in W^{1,p}(\mathcal{O}(\Omega_h^n))$, and $U \in W^{2,p}(\mathcal{O}(\Omega_h^n))$, where $\frac{1}{p} + \frac{1}{q} = 1$, there holds:*

$$\begin{aligned} \int_{\Omega_h^n} |(T \circ \boldsymbol{\Phi}) : R - T : R| \, d\boldsymbol{x} &\lesssim h^{q+1} \|\nabla T\|_{L^p(\mathcal{O}(\Omega_h^n))} \|R\|_{L^q(\Omega_h^n)}, \\ \int_{\Gamma_h^n} |(U \circ \boldsymbol{\Phi}) : S - U : S| \, dS &\lesssim h^{q+1} \|U\|_{W^{2,p}(\mathcal{O}(\Omega_h^n))} \|S\|_{L^q(\Gamma_h^n)}. \end{aligned} \tag{140}$$

Lemma 11. *Given $f \in L^1(\Omega_h^n)$ and $g \in L^1(\Gamma_h^n)$, there holds:*

$$\left| \int_{\Omega_h^n} f \det(\nabla \boldsymbol{\Phi}) - f d\boldsymbol{x} \right| \lesssim h^q |f\|_{L^1(\Omega_h^n)}, \quad \left| \int_{\Gamma_h^n} g \mu_h - g d\boldsymbol{x} \right| \lesssim h^q \|g\|_{L^1(\Gamma_h^n)}. \tag{141}$$

Lemma 12. *Given $\boldsymbol{v} \in L^p(\Omega_h^n)$, then we have the following:*

$$\|(\nabla \boldsymbol{\Phi}^T)^{-1} \boldsymbol{v} - \boldsymbol{v}\|_{L^p(\Omega_h^n)} \lesssim h^q \|\boldsymbol{v}\|_{L^p(\Omega_h^n)}. \tag{142}$$

This result is taken from [43, Cor. 4.13].

Lemma 13. *Let $\boldsymbol{R}(\boldsymbol{a}, t) := \boldsymbol{a} + tY(\boldsymbol{a})$, for all t in a bounded, open interval I, and a.e. $\boldsymbol{a} \in \mathbb{R}^d$, where $Y \in [W^{1,\infty}(\mathbb{R}^d)]^d$. Assume that $\|Y\|_{W^{1,\infty}}$ is sufficiently small so that for all $t \in I$, $\nabla_{\boldsymbol{a}} \boldsymbol{R}(\boldsymbol{a}, t)$ is a matrix with positive determinant and $|\nabla_{\boldsymbol{a}} \boldsymbol{R}(\boldsymbol{a}, t)| = O(1)$, i.e. $\boldsymbol{R}(\cdot, t) : \mathbb{R}^d \to \mathbb{R}^d$ is a differentiable homeomorphism for all $t \in I$. Now let $g \in L^p(\mathbb{R}^d)$, and define $q : \mathbb{R}^d \times I \to \mathbb{R}$ by $q(\boldsymbol{a}, t) = g \circ \boldsymbol{R}(\boldsymbol{a}, t)$. Then, $q \in L^p(\mathbb{R}^d \times I)$ and $\|q\|_{L^p(\mathbb{R}^d \times I)} \leq C|I|^{1/p} \|g\|_{L^p(\mathbb{R}^d)}$ for some bounded constant C.*

A.3 Other Results

The following lemma from [47] is needed in the analysis.

Lemma 14. *(Discrete Grönwall Inequality) Let* $\{u_n\}$ *satisfy*

$$u_k \leq \alpha_k + \sum_{n=0}^{k-1} \beta_n u_n, \quad \forall k \geq 0, \tag{143}$$

where α_k *is nondecreasing with respect to* k *and* $\beta_k \geq 0$ *for all* $k \geq 0$*. Then it follows that*

$$u_k \leq \alpha_k \exp\left(\sum_{n=0}^{k-1} \beta_n\right). \tag{144}$$

References

[1] U. A. Acar, B. Hudson, G. L. Miller, and T. Phillips. Svr: Practical engineering for a fast 3D meshing algorithm. In *16th International Meshing Roundtable*, 2007.

[2] T. Araki and H. Tanaka. Colloidal aggregation in a nematic liquid crystal: Topological arrest of particles by a single-stroke disclination line. *Phys. Rev. Lett.*, 97:127801, Sep 2006.

[3] I. Bajc, F. Hecht, and S. Žumer. A mesh adaptivity scheme on the Landau–de Gennes functional minimization case in 3D, and its driving efficiency. *Journal of Computational Physics*, 321:981 – 996, 2016.

[4] G. Barbero and G. Durand. On the validity of the rapini-papoular surface anchoring energy form in nematic liquid crystals. *J. Phys. France*, 47(12):2129–2134, 1986.

[5] A. N. Beris and B. J. Edwards. *Thermodynamics of Flowing Systems: With Internal Microstructure*, volume 36 of *Oxford Engineering Science Series*. Oxford University Press, 1st edition, 1994.

[6] H. K. Bisoyi and S. Kumar. Liquid-crystal nanoscience: an emerging avenue of soft self-assembly. *Chem. Soc. Rev.*, 40:306–319, 2011.

[7] J. P. Borthagaray and S. W. Walker. Chapter 5 - the Q-tensor model with uniaxial constraint. In A. Bonito and R. H. Nochetto, editors, *Geometric Partial Differential Equations - Part II*, volume 22 of *Handbook of Numerical Analysis*, pages 313 – 382. Elsevier, 2021.

[8] J. Bronson, J. Levine, and R. Whitaker. Lattice cleaving: Conforming tetrahedral meshes of multimaterial domains with bounded quality. In X. Jiao and J.-C. Weill, editors, *Proceedings of the 21st International Meshing Roundtable*, pages 191–209. Springer Berlin Heidelberg, 2013.

[9] E. Burman. Ghost penalty. *Comptes Rendus Mathematique*, 348(21):1217–1220, 2010.

[10] E. Burman, S. Claus, P. Hansbo, M. G. Larson, and A. Massing. Cutfem: Discretizing geometry and partial differential equations. *International Journal for Numerical Methods in Engineering*, 104(7):472–501, 2015.

[11] E. Burman and P. Hansbo. Fictitious domain finite element methods using cut elements: II. a stabilized Nitsche method. *Applied Numerical Mathematics*, 62(4):328–341, 2012. Third Chilean Workshop on Numerical Analysis of Partial Differential Equations (WONAPDE 2010).

[12] E. Burman, P. Hansbo, M. G. Larson, and S. Zahedi. Cut finite element methods for coupled bulk–surface problems. *Numerische Mathematik*, 133(2):203–231, 2016.

[13] S. Changizrezaei and C. Denniston. Heterogeneous colloidal particles immersed in a liquid crystal. *Phys. Rev. E*, 95:052703, May 2017.

[14] M. Conradi, M. Ravnik, M. Bele, M. Zorko, S. Žumer, and I. Muševič. Janus nematic colloids. *Soft Matter*, 5:3905–3912, 2009.

[15] T. Davis and E. Gartland. Finite element analysis of the Landau-de Gennes minimization problem for liquid crystals. *SIAM Journal on Numerical Analysis*, 35(1):336–362, 1998.

[16] P. G. de Gennes and J. Prost. *The Physics of Liquid Crystals*, volume 83 of *International Series of Monographs on Physics*. Oxford Science Publication, Oxford, UK, 2nd edition, 1995.

[17] L. C. Evans. *Partial Differential Equations*. American Mathematical Society, Providence, Rhode Island, 1998.

[18] A. Friedman. *Partial Differential Equations of Parabolic Type*. Dover, 2008.

[19] E. C. Gartland Jr, P. Palffy-Muhoray, and R. S. Varga. Numerical minimization of the Landau-de Gennes free energy: Defects in cylindrical capillaries. *Molecular Crystals and Liquid Crystals*, 199(1):429–452, 1991.

[20] Z. Geng, A. Roy, and A. Zarnescu. Global existence of weak solutions for a model of nematic liquid crystal-colloidal interactions. *SIAM Journal on Mathematical Analysis*, 56(4):4324–4355, 2024.

[21] J. W. Goodby. *Handbook of Visual Display Technology (Editors: Chen, Janglin, Cranton, Wayne, Fihn, Mark)*, chapter Introduction to Defect Textures in Liquid Crystals, pages 1290–1314. Springer, 2012.

[22] Gross, Sven, Olshanskii, Maxim A., and Reusken, Arnold. A trace finite element method for a class of coupled bulk-interface transport problems. *ESAIM: M2AN*, 49(5):1303–1330, 2015.

[23] M. E. Gurtin. *Thermomechanics of Evolving Phase Boundaries in the Plane*. Oxford Mathematical Monographs. Oxford Science Publication, 1993.

[24] P. Hansbo, M. G. Larson, and K. Larsson. *Cut Finite Element Methods for Linear Elasticity Problems*, volume 121 of *Lecture Notes in Computational Science and Engineering*, pages 25–63. Springer International Publishing, 2017.

[25] P. Hansbo, M. G. Larson, and S. Zahedi. A cut finite element method for a stokes interface problem. *Applied Numerical Mathematics*, 85:90–114, 2014.

[26] A. Hicks. *Modeling and Numerical Analysis of the Cholesteric Landau–de Gennes Model*. PhD thesis.

[27] A. L. Hicks and S. W. Walker. Modelling and simulation of the cholesteric landau–de gennes model. *Proceedings of the Royal Society A: Mathematical, Physical and Engineering Sciences*, 480(2292):20230813, 2024.

[28] J. Hoogboom, J. A. Elemans, A. E. Rowan, T. H. Rasing, and R. J. Nolte. The development of self-assembled liquid crystal display alignment layers. *Philosophical Transactions of the Royal Society of London A: Mathematical, Physical and Engineering Sciences*, 365(1855):1553–1576, 2007.

[29] B. M. Klingner and J. R. Shewchuk. Agressive tetrahedral mesh improvement. In *In Proceedings of the 16th International Meshing Roundtable*, pages 3–23, Seattle, Washington, October 2007.

[30] N. V. Krylov. *Lectures on Elliptic and Parabolic Equations in Sobolev Spaces*. Graduate Studies in Mathematics. American Mathematical Society, 2008.

[31] O. V. Kuksenok, R. W. Ruhwandl, S. V. Shiyanovskii, and E. M. Terentjev. Director structure around a colloid particle suspended in a nematic liquid crystal. *Phys. Rev. E*, 54:5198–5203, Nov 1996.

[32] P. Lederer, C.-M. Pfeiler, C. Wintersteiger, and C. Lehrenfeld. Higher order unfitted fem for Stokes interface problems. *PAMM*, 16(1):7–10, 2016.

[33] C. Lehrenfeld, F. Heimann, J. Preuss, and H. von Wahl. ngsxfem: Add-on to NGSolve for geometrically unfitted finite element discretizations. *Journal of Open Source Software*, 6(64):3237, 2021.

[34] C. Lehrenfeld and M. Olshanskii. An Eulerian finite element method for PDEs in time-dependent domains. *ESAIM: Mathematical Modelling and Numerical Analysis*, 53(2):585–614, 2019.

[35] A. Massing, M. G. Larson, A. Logg, and M. E. Rognes. A stabilized Nitsche fictitious domain method for the Stokes problem. *J. Sci. Comput.*, 61(3):604–628, Dec. 2014.

[36] H. Mori, J. Eugene C. Gartland, J. R. Kelly, and P. J. Bos. Multidimensional director modeling using the Q-tensor representation in a liquid crystal cell and its application to the π-cell with patterned electrodes. *Japanese Journal of Applied Physics*, 38(1R):135–146, 1999.

[37] N. J. Mottram and C. J. P. Newton. Introduction to Q-tensor theory. *ArXiv e-prints*, Sept. 2014.

[38] I. Muševič. *Liquid Crystal Colloids*. Soft and Biological Matter. Springer Cham, 1 edition, 2017.

[39] M. Paicu and A. Zarnescu. Energy dissipation and regularity for a coupled navier-stokes and Q-tensor system. *Archive for Rational Mechanics and Analysis*, 203(1):45–67, 2012.

[40] M. Ravnik and S. Žumer. Landau-degennes modelling of nematic liquid crystal colloids. *Liquid Crystals*, 36(10-11):1201–1214, 2009.

[41] J. Schöberl. C++11 implementation of finite elements in NGSolve. Technical Report ASC-2014-30, Institute for Analysis and Scientific Computing, September 2014.

[42] A. A. Shah, H. Kang, K. L. Kohlstedt, K. H. Ahn, S. C. Glotzer, C. W. Monroe, and M. J. Solomon. Self-assembly: Liquid crystal order in colloidal suspensions of spheroidal particles by direct current electric field assembly (small 10/2012). *Small*, 8(10):1551–1562, 2012.

[43] J. T. Shahan. *Unfitted Finite Element Methods for Shape Optimization and Liquid Crystals*. PhD thesis.

[44] J. T. Shahan and S. W. Walker. Exact shape derivatives with unfitted finite element methods. *Journal of Numerical Mathematics*, 2025.

[45] A. M. Sonnet and E. Virga. *Dissipative Ordered Fluids: Theories for Liquid Crystals*. Springer, New York, NY, 2012.

[46] T. M. Surowiec and S. W. Walker. Optimal control of the Landau–de Gennes model of nematic liquid crystals. *SIAM Journal on Control and Optimization*, 61(4):2546–2570, 2023.

[47] V. Thomée. *Galerkin Finite Element Methods for Parabolic Problems*. Springer Series in Computational Mathematics. Springer Berlin, Heidelberg, 2nd edition, 2006.

[48] S. Čopar, U. Tkalec, I. Muševič, and S. Žumer. Knot theory realizations in nematic colloids. *Proceedings of the National Academy of Sciences*, 112(6):1675–1680, 2015.

[49] E. G. Virga. *Variational Theories for Liquid Crystals*, volume 8. Chapman and Hall, London, 1st edition, 1994.

[50] H. von Wahl, T. Richter, and C. Lehrenfeld. An unfitted Eulerian finite element method for the time-dependent Stokes problem on moving domains. *IMA Journal of Numerical Analysis*, 42(3):2505–2544, 07 2021.

[51] J. Zhao and Q. Wang. Semi-discrete energy-stable schemes for a tensor-based hydrodynamic model of nematic liquid crystal flows. *Journal of Scientific Computing*, 68(3):1241–1266, Sep 2016.

[52] J. Zhao, X. Yang, J. Shen, and Q. Wang. A decoupled energy stable scheme for a hydrodynamic phase-field model of mixtures of nematic liquid crystals and viscous fluids. *Journal of Computational Physics*, 305:539 – 556, 2016.